
Faith and Fate: Limits of Transformers on Compositionality

Nouha Dziri^{1*}, Ximing Lu^{1,2*}, Melanie Sclar^{2*}, Xiang Lorraine Li^{1†}, Liwei Jiang^{1,2 †}, Bill Yuchen Lin¹, Peter West^{1,2}, Chandra Bhagavatula¹, Ronan Le Bras¹, Jena D. Hwang¹, Soumya Sanyal³, Sean Welleck^{1,2}, Xiang Ren^{1,3}, Allyson Ettinger^{1,4}, Zaid Harchaoui^{1,2}, Yejin Choi^{1,2}

¹ Allen Institute for Artificial Intelligence ²University of Washington

³University of Southern California ⁴University of Chicago

nouhad@allenai.org, ximinglu@allenai.org, msclar@cs.washington.edu

Abstract

Transformer large language models (LLMs) have sparked admiration for their exceptional performance on tasks that demand intricate multi-step reasoning. Yet, these models simultaneously show failures on surprisingly trivial problems. This begs the question: Are these errors incidental, or do they signal more substantial limitations? In an attempt to demystify Transformers, we investigate the limits of these models across three representative *compositional* tasks—multi-digit multiplication, logic grid puzzles, and a classic dynamic programming problem. These tasks require breaking problems down into sub-steps and synthesizing these steps into a precise answer. We formulate compositional tasks as computation graphs to systematically quantify the level of complexity, and break down reasoning steps into intermediate sub-procedures. Our empirical findings suggest that Transformers solve compositional tasks by reducing multi-step compositional reasoning into linearized subgraph matching, without necessarily developing systematic problem-solving skills. To round off our empirical study, we provide theoretical arguments on abstract multi-step reasoning problems that highlight how Transformers’ performance will rapidly decay with increased task complexity.

1 Introduction

“It was the epoch of belief, it was the epoch of incredulity.” – Charles Dickens, A Tale of Two Cities

Large-scale Transformers such as ChatGPT [41] and GPT-4 [42] demonstrate unprecedented capabilities [41, 57, 9, 12, 66], even noted as “sparks of AGI” [10]. In stark contrast, the same models sometimes struggle with simple, intuitive tasks [8, 45, 35]. For instance, humans can solve 3-digit by 3-digit multiplication arithmetic after learning basic calculation rules [19, 29]. Yet, off-the-shelf ChatGPT and GPT4 achieve only 55% and 59% accuracies on this task, respectively (§3).

The striking discrepancy between the impressive successes of Transformers on *seemingly complex* tasks and the astonishing failures on *seemingly trivial* tasks spark critical open questions about how to faithfully interpret their mixed capabilities. Under what conditions do Transformers succeed, fail, and why? What types of errors do they make? Can Transformers uncover implicit problem-solving rules or be taught to follow reasoning paths?

* First co-authors.

† Second co-authors.

Seeking thorough answers to these questions remains an open research challenge. However, we offer novel insights into the fundamental limits of Transformer LLMs, centered around *compositional problems* that require strict multi-hop reasoning to derive correct predictions. Applying step-by-step reasoning is fundamental to human intelligence [52, 51]. These compositional problems present compelling challenges for AI systems as they require combining basic reasoning operations to follow computational paths that arrive at unique correct solutions. In particular, we study three straightforward and flexible representative compositional tasks: long-form multiplication, logic grid puzzles (i.e., Einstein’s puzzle [44]), and a classic dynamic programming problem.

We propose two hypotheses. **First**, Transformers solve compositional tasks by reducing multi-step compositional reasoning into linearized path matching. This contrasts with the systematic multi-step reasoning approach that learns to apply underlying *computational rules* required for building correct answers [54, 32, 24]. Shortcut learning [26] via pattern-matching may yield fast correct answers when similar compositional patterns are available during training but does not allow for robust generalization to uncommon or complex examples. **Second**, due to error propagation, Transformers may have inherent limitations on solving high-complexity compositional tasks that exhibit novel patterns. Errors in the early stages of the computational process can lead to substantial compounding errors in subsequent steps, preventing models from finding correct solutions.

To investigate our hypotheses, we formulate compositional tasks as *computation graphs*. These graphs break down problem-solving into submodular functional steps, enabling structured measurements of complexity and verbalization of computational steps as input sequences to language models. Moreover, we leverage information gain to predict patterns that models are likely to learn based on the underlying task distribution without the need to perform full computations within the graph.

Empirical results show that training on task-specific data leads to near-perfect performance on in-domain instances and under low compositional complexity, but fails drastically on instances outside of this region. This substantial gap suggests that systematic problem-solving capabilities do not emerge from maximum likelihood training [5] on input-output sequences, even when prompted or trained with human-like reasoning steps (i.e., a linearization of computation graphs; §3.1). Models’ success can be attributed, in part, to their exposure to training examples sub-graphs that involve the same computations required for solving test examples (see Section 3.2.2) In order to gain a deeper understanding of models’ failures, we conduct a comprehensive analysis by decomposing their computation graphs and examining different error types. We find that while models can memorize single-step operations, they fail to compose them into correct reasoning paths, suggesting that they mostly make predictions based on shallow, rote learning rather than a deep, holistic task understanding (§3.2.3). Importantly, we provide theoretical evidence of exponential error accumulation using abstract compositional tasks. All tasks analyzed empirically in this paper are instantiations of these abstractions (§4). We argue that Transformers could be inherently limited in solving compositionally complex tasks out-of-the-box.

As Transformers continue to make tangible real-world impacts, it is pressing to interpret their remarkable performance critically. Our work takes a realistic look at the limitations of Transformers in the context of compositional tasks. To shed light on practical future steps, we identify directions for addressing these limitations, such as using Transformers for tasks that could be decomposed into few reasoning steps, tasks where evaluation may afford some leniency, and using Transformers in combination with planning modules or refinement methods to improve their generations. To advance language AI, fundamental innovations are required to address or complement these limitations.

2 Measuring Limitations of Transformers in Compositional Tasks

Human problem-solving skills can be conceptualized as a graph structure, where each vertex represents a partial solution and the edges represent operators that can be applied to modify these solutions. As we will outline next and illustrate in Figure 1, we use computation graphs and corresponding metrics to methodically evaluate Transformers’ reasoning abilities.

2.1 Computation Graph Definition

Let A be a deterministic algorithm (function), and let \mathcal{F}_A be a set of primitives (functions) the algorithm uses in its execution. Assuming the inputs x to algorithm A are given, we define $A(x)$ ’s

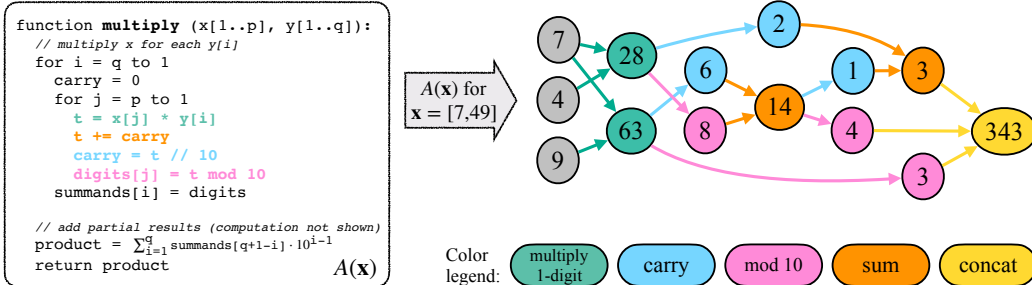


Figure 1: Transformation of an algorithm A to its computational graph $G_{A(\mathbf{x})}$. The depicted example is of long-form multiplication algorithm A , for inputs $\mathbf{x} = [7, 49]$ (i.e. computing 7×49).

static computation graph $G_{A(\mathbf{x})}$. $G_{A(\mathbf{x})} = (V, E, s, op)$ is a directed acyclic graph. Nodes V represent all variables’ values during A ’s execution: each node $v \in V$ has a value $s(v) \in \mathbb{R}$ associated. Edges E represent the function arguments involved in some computation: for each non-source node $v \in V$, let $U = \{u_1, \dots, u_j\} \subset V$ be its parent nodes. Then, $s(v) = f(u_1, \dots, u_j)$ for some $f \in \mathcal{F}_A$. Since each node v is uniquely defined by the computation of a single primitive f , we define $op : V \rightarrow \mathcal{F}_A$ as $op(v) = f$.

Let $S \subset V$ be the source nodes of $G_{A(\mathbf{x})}$ and without loss of generality, let $o \in V$ be its sole leaf node. By definition, $S \equiv \mathbf{x}$ and $A(\mathbf{x}) = s(o)$, representing the input and output of A respectively.

To be able to train and evaluate a language model’s ability to follow algorithm A we must linearize $G_{A(\mathbf{x})}$. Since we only consider autoregressive models, this linearization must also be a topological ordering.

2.2 Quantifying Compositional Complexity using Graph Metrics

A ’s representation as a computation graph $G_{A(\mathbf{x})}$ enables measuring task complexity from many angles.

We define a node $v \in V$ ’s *layer number* as the length of the longest path from a source node to v in the directed acyclic graph $G_{A(\mathbf{x})}$. We then define the **reasoning depth** as the largest layer number in the graph. In computation graphs, reasoning depth is a proxy for the maximum level of multi-hop reasoning required to solve the task.

Let $d_S : V \rightarrow \mathbb{N}_0$ be the shortest distance to any of G ’s source nodes $S \subset V$. We define the **reasoning width** of a graph as the mode of $\{d(v) : v \in V\}$. This metric aims to measure the maximum number of variables required to maintain in parallel during the computation. Relatedly, we also define the **average parallelism** of a graph as the ratio between $|V|$ and its reasoning depth. This aims to compute the average width in computation through the graph, and not just in its mode.

2.3 Predicting Surface Patterns through Relative Information Gain

When evaluating model performance, we may observe partially correct answers even in an overall incorrect response. To understand model strategies in these partial successes, we use Relative Information Gain to predict surface patterns that models are likely to recognize. We represent task T as a distribution $(X_1, \dots, X_n, Y_1, \dots, Y_m)$ and measure the amount of (normalized) information gained about an output element Y_j by observing a subset of input random variables $X \subset \{X_1, \dots, X_n\}$:

$$\text{RelativeIG}(Y_j, X) = \frac{H(Y_j) - H(Y_j | X)}{H(Y_j)} \in [0, 1] \quad (1)$$

RelativeIG may be used to analyze the influence of any node in the computation graph (as defined in §2.1) with respect to a set of its ancestors; in particular, output nodes with respect to input nodes.

2.4 Exploring Three Representative Compositional Tasks: Definitions

Multiplication Multi-digit multiplication requires executing operations with numerical symbols based on procedural rules [29]. This task has multiple algorithmic solutions; in constructing computa-

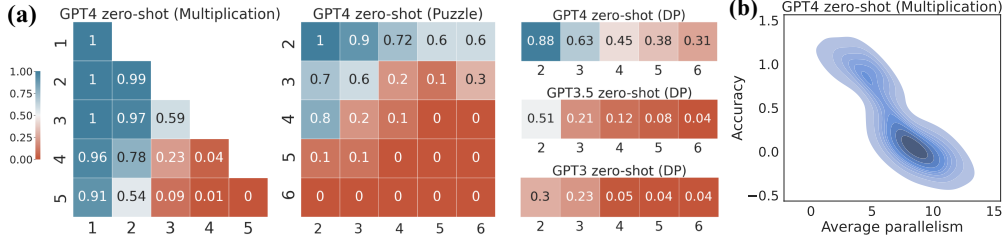


Figure 2: (a) **Zero-shot accuracy**. Axes refer to problem sizes (number of digits in multiplication, number of houses and attributes in puzzle, and sequence length in the DP task). Transformers’ accuracy decreases to near zero as task complexity increases, measuring task complexity by the problem size. (b) **Average parallelism** negatively correlates with accuracy.

tion graphs, we use the well-known $O(k_1 k_2)$ long-form multiplication algorithm for computing $x \cdot y$, where x has $k_1 \leq 5$ digits and y has $k_2 \leq 5$ digits in base 10. See §A.1 for data construction details.

To instantiate $G_{A(x)}$, let $\mathcal{F}_A = \{\text{one-digit multiplication, sum, mod 10, carry over, concatenation}\}$. Source nodes S are digits of input numbers, leaf node o is the final output, and intermediate nodes v are partial results generated during execution of the long-form multiplication algorithm (see Figure 1).

Einstein’s Puzzle Einstein’s puzzle is a well-known logic puzzle often used as a benchmark for solving constraint satisfaction problems [44]. It involves a list of houses with different attributes (e.g., owner’s name, pets), and the goal is to determine which attributes belong to each house by combining a set of pre-defined natural language clues or constraints. The solution to the puzzle is a matrix of size $K \times M$, where K represents the number of houses and M the number of attributes. As K and M increase, synthesizing different partial solutions that satisfy individual constraints becomes highly compositionally complex. To construct the computation graph, we consider a greedy algorithm that iteratively eliminates possible solutions by filling at least one cell each time. It deterministically fills the cell(s) that requires the minimum number of clues among all current unfilled cells. We refer to this as the *elimination function*. See §A.2 for examples, data construction, and algorithm details.

To instantiate $G_{A(x)}$, let $\mathcal{F}_A = \{\text{elimination function}\}$. The source nodes are the clues, all intermediate nodes are partially-filled matrices, and the output node is a fully-filled solution matrix.

Dynamic Programming Problem Dynamic programming (DP) recursively breaks down complex problems into simpler sub-problems, so problems solved using this technique are compositional. We analyze a classic relaxation of the NP-complete Maximum Weighted Independent Set problem [34]: *Given a sequence of integers, find a subsequence with the highest sum, such that no two numbers in the subsequence are adjacent in the original sequence.* This relaxation may be solved in $O(n)$ time using DP. See the solution in §A.3. In the experiments, we restrict each integer to the $[-5, 5]$ range.

To instantiate $G_{A(x)}$, let $\mathcal{F}_A = \{\text{equals, and, not, indicator function, sum, max}\}$. Source nodes are elements of the input list, and the output node is a list that for each element indicates whether it should be selected. We select an $O(n)$ algorithm since $G_{A(x)}$ ’s size is proportional to A ’s complexity.

3 Testing the Limits of Transformers: Empirical Evidence

Experimental Setup To understand the capabilities of LLMs, we evaluate GPT3 (text-davinci-003) [9], ChatGPT (GPT-3.5-turbo) [41] and GPT4 (gpt-4) [42] using zero-shot, few-shot, and finetuning techniques. To enable the generation of computation graphs beyond the final answers, we use the concept of *scratchpads* [40]. Scratchpads are a verbalization of the computation graphs (i.e., a linearized representation of a topological ordering of $G_{A(x)}$). Overall, we consider *question-answer* and *question-scratchpad* formats for few-shot and finetuning settings to gauge models’ capabilities for learning with and without explicit reasoning. See details of additional models and experimental configurations in §B and examples of scratchpad in §A.

3.1 Testing the Limits of Transformers with Zero-shot, Few-shot and Finetuning

Limits of Transformers in zero- and few-shot settings To investigate the inherent problem-solving capabilities of LLMs, we begin by analyzing models’ zero-shot and few-shot performances on our compositional tasks. As shown in Figure 2, task performances deteriorate significantly from near perfection to zero with increasing complexity when measured by either problem size (Figure 2(a)) or average parallelism (Figure 2(b)). The trend remains the same for few-shot prompting (see §B.2). These results indicate that pre-training is in fact not sufficient to teach models how to combine basic operations to solve compositional problems, especially as problems grow more complex.

Limits of Transformers with question-answer training The limited performance of models may be attributed to the lack of task-specific data during pre-training. To fully bring out models’ potentials in solving these tasks, we next exhaustively finetune GPT3 with question-answer pairs. In multiplication and DP, we finetune models with all enumerations of questions up to the maximum problem size³ within reasonable training budget, leaving out 10% for validation and 10% for testing. In puzzles, we train on a subset of all instances up to $(K, M) \leq (4, 4)$ due to combinatorial explosion. We separately finetune GPT3 models on $\sim 1.8M$ multiplication pairs, $\sim 142K$ DP pairs, and $\sim 41K$ puzzle pairs (see details in §B.3). Additionally, to examine problems of different complexity, we consider different training splits based on the depth and width of computation graphs.

Figure 3 and Figure 4a show high accuracy for examples with splits seen during training, i.e., *in-domain*. However, the performance sharply declines when evaluating unseen splits during training, i.e., *out-of-domain (OOD)*. Similar trends hold in all tasks (see § B.3), suggesting that systematic problem-solving capabilities do not emerge via exhaustive training on task-specific data.

Limits of Transformers with explicit scratchpad training

Next, we test whether we can explicitly teach models the required computational operations via *scratchpads*. To do so, we finetune GPT3 with question-scratchpad pairs for all tasks. We considered the same distribution splits as before. The results, presented in Figure 4b, show that once again GPT3 achieves near-perfect performance on in-distribution, but fails entirely in generalizing to OOD cases—in particular, wider or deeper computation graphs. These results indicate that even when training directly with guidance on the computation steps, models still fail to learn component operations in a generalizable manner. This observation holds for all tasks (See details in § B.4). These findings suggest that the autoregressive characteristic of Transformers, which forces them to tackle problems sequentially, presents a fundamental challenge that cannot be resolved by instructing the model to generate a step-by-step solution. Instead, models face the fundamental challenge of simply depending on a greedy process of producing the next word to make predictions without a rigorous global understanding of the task.

3.2 Breaking Down Successes and Failures of Transformers

3.2.1 Information Gain Explains Where Transformers Partially Excel

At times Transformers predict partially correct answers even when the overall response is incorrect. We speculate that this may be due to particularities in the task distribution that allow for guessing partial answers without performing the full multi-step reasoning that the task requires.

Using relative information gain (defined in §2.3), we can predict surface patterns that a model is likely to learn and contrast them empirically. For multiplication, relative information gain shows that the first digit (two digits) of the output highly correlates with the first digit (two digits) of each input number (see §C.1). Hence, this spurious pattern is likely to be learned by a model. Similarly, the prediction of the last digit (or two digits) of the output is observed to solely rely on the last digit (or

³We consider all k_1 -by- k_2 digit multiplications with $1 \leq k_1, k_2 \leq 4$ and $k_1 \cdot k_2 \leq 9$; and all DP problems up to 5 elements. We selected sizes based on budget constraints for GPT3 finetuning, see §B.3 for cost details.

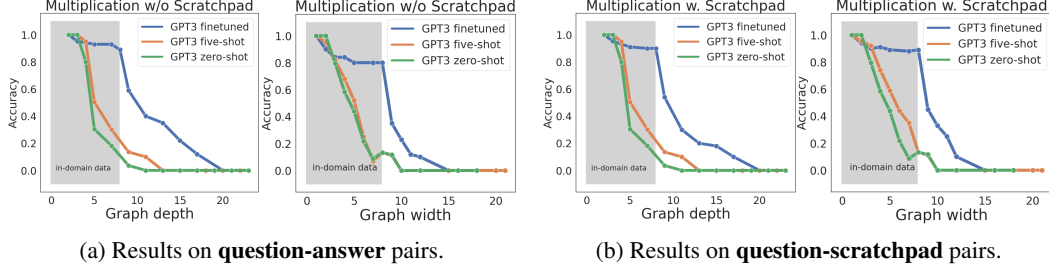


Figure 4: **GPT3 finetuning and prompting accuracy** on different data splits. Although the in-distribution performance is almost perfect, GPT3 exhibits poor generalization with increasing graph depth and width. Refer to §B.3 and §B.4 for results on the puzzle and DP tasks.

two digits) of each input number. This pattern holds true due to the principles of modulo arithmetic, which ensures the validity of this relationship in all cases. Empirically, we verify that models indeed learn the patterns we predicted and other patterns as well (e.g., order of magnitude of the answer, number of trailing zeros for multiplication) in all the settings with and without scratchpad. See details for multiplication, plus dynamic programming task analysis in §C.

These experiments suggest that if an output element heavily relies on a single or a small set of input features, Transformers are likely to recognize such correlation during training and directly map these input features to predict the output element in testing, without going through the rigorous multi-hop reasoning and giving a false illusion of performing compositional reasoning.

3.2.2 Transformers Reduce Multi-Step Compositional Reasoning into Linearized Subgraph Matching

We now explore whether models’ correct predictions on unseen test data are due to learning the underlying algorithm or, instead, explainable by exposure to similar training examples. We hypothesize that, beyond simple memorization, Transformers largely rely on pattern matching for solving these tasks. To test this, we calculate the average frequency with which partial computations needed to solve an instance appear in the training data, for both correctly and wrongly predicted examples.

Given a model-generated computation graph $\hat{G}_{A(\mathbf{x})}$ we analyze how often the full computation of each node $v \in \hat{V}$ is seen in training. We define v ’s *full computation* as the subgraph induced by all ancestors of v including v , denoted $FC_{\hat{G}_{A(\mathbf{x})}}(v)$. We say that $FC_{\hat{G}_{A(\mathbf{x})}}(v)$ is seen during training if $FC_{\hat{G}_{A(\mathbf{x})}}(v) \equiv FC_{G_{A(\mathbf{x}')}}(w)$ for some computation graph $G_{A(\mathbf{x}'')}$ in training, and for some $w \in V$. We characterize complexity of a full computation subgraph by its depth, as defined in §2.1.

Figure 5 shows that full computation subgraphs appear significantly more frequently in the training data for correctly predicted test examples than for incorrectly predicted ones, for both the multiplication and DP task (both frequencies tend to zero for large depths since we ensured a disjoint train/test split). This high correlation suggests that pattern matching—and not general reasoning capabilities—may be the cause behind correct model outputs. This type of learning could be largely effective when the compositional complexity of tasks is low but it becomes less efficient when tasks are increasingly complex. This may elucidate the observed performance gain in low-complexity and in-domain cases and the striking performance drop in OOD and highly complex cases.

3.2.3 What Types of Errors do Transformers Make at Different Reasoning Depths?

For clearer understanding of where Transformers fall short, we analyze the types of errors that transformers make for nodes at different layers in the computation graph. For every input \mathbf{x} , we compare the ground truth computation graph $G_{A(\mathbf{x})}$ with the (possibly incorrect) model-generated computation graph $\hat{G}_{A(\mathbf{x})}$. We consider a node v as having a *correct value* if and only if $s(v) = \hat{s}(v)$.⁴. We consider a node v to be derived from a *correct computation* if given that $U = \{u_1, \dots, u_k\}$ are the immediate predecessors of v in $\hat{G}_{A(\mathbf{x})}$ and that $\hat{o}_p(v) = f$, we have that $f(u_1, \dots, u_k) = \hat{s}(v)$.

⁴If a node v does not appear in the ground truth graph G , we consider it to have an incorrect value.

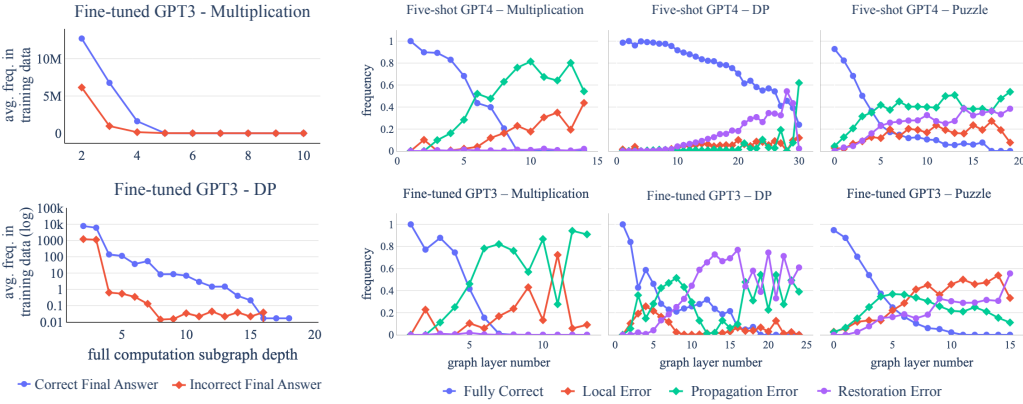


Figure 5: Average frequency in training data w.r.t. the subgraph depth, grouped by final answer.

Figure 6: Ratio of nodes in each of the four correct/error categories which test examples’ full computation graph appear in the training data w.r.t. the subgraph depth, grouped by final answer.

Note that the notion of correct computation is independent of G , and that a node v derived from a correct computation may not have the correct value if an error occurred in some of its ancestors.

We classify each node $v \in \hat{V}$ into one of four categories. Node v is **fully correct** if v and its ancestors have correct values and are derived from correct computations. If a node v is not fully correct, its error can be of the following types: v has a **local error** if its parent nodes have correct values but v is derived from an incorrect computation (i.e., a one-hop reasoning error); v has a **propagation error** if v is derived from a correct computation but some of its parent nodes have incorrect values; v has a **restoration error** if it has a correct value but is derived from an incorrect computation.

Figure 6 shows results for few-shot GPT4 and fine-tuned GPT3 with scratchpad, with respect to graph layer number for each node. In all settings, the ratio of fully correct nodes is almost perfect but sharply decreases toward zero with increasing graph layers. Moreover, the ratio of propagation errors is usually higher than the ratio of local errors. Both phenomena suggest that models are able to correctly perform single-step reasoning, potentially due to memorizing such single-step operations during training, but fail to plan and compose several of these steps for an overall correct reasoning.

Both the DP and the puzzle tasks have a high ratio of restoration errors, suggesting memorization since correct outputs are produced despite incorrect computations. There are signs of memorization even when restoration errors are near zero: 82.3% of the final correct answers for 4-digit by 2-digit multiplications (a setting unseen during training) had at least one error in the computation graph, but still produced correct answers. These patterns are possibly due to high frequency of (input, output) multiplication pairs in the pretraining data, in contrast to intermediate reasoning steps.

4 Error Propagations: The Theoretical Limits

Experiments (§3) highlight the limitations of current Transformers in handling complex, multi-step reasoning tasks. Concretely, we show that errors rapidly escalate as the problem size grows (§3.2.3). In this section, we aim to provide theoretical insights into why these models can perform significantly worse in compositional tasks as the problem size increases. We argue using stylized examples that transformers may be too limited to solve compositionally complex tasks.

Algorithms designed to solve compositional tasks typically involve multiple independent applications of a function and/or iterated applications of the same function. A Transformer executing such an algorithm acts as an estimator of these functions. In this context, we examine the probability of such an estimator reaching the correct answer as the problem size increases. We first consider a scenario where a Transformer estimates an algorithm requiring n independent applications of a function:

Proposition 4.1 (informal). *Let f_n involve the combination h_n of n independent applications of a function g . Let $\hat{f}, \hat{g}, \hat{h}_n$ be their estimators. Assume h_n has low collision and that \hat{h}_n is a perfect estimator of h_n . If $\mathbb{P}(g \neq \hat{g}) > 0$ where \hat{g} 's errors are independent, then $\mathbb{P}(f_n \neq \hat{f}_n)$ tends to 1 as n increases.*

Proof sketch. Derive an upper bound for $\mathbb{P}(f_n = \hat{f}_n)$ by using the law of total probability on the event that the estimations \hat{g} were correct for all of the n independent applications. Show it converges to zero as $n \rightarrow +\infty$. See §D.1 for a formal statement and proof derivation. \square

Proposition 4.1's proof shows the rate of convergence is exponential, thus concluding that transformers will rapidly fail with increasing n . Let's now analyze the iterated application function scenario.

Proposition 4.2 (informal). *Let $f_n(x) = g^n(x)$ involve the repeated application of g . Assume that the probability of recovering from a mistake due to the randomness of applying the estimator on an incorrect input has probability at most c . If $\mathbb{P}(g \neq \hat{g}) = \epsilon > 0$, then $\liminf_{n \rightarrow +\infty} \mathbb{P}(f_n \neq \hat{f}_n) = 1 - c/(c + \epsilon)$.*

Proof sketch. Let $s_n := \mathbb{P}(f_n = \hat{f}_n)$, where $s_1 = 1 - \epsilon$ by definition. Derive $s_n \leq (1 - \epsilon - c) \cdot s_{n-1} + c$ using law of total probability. Then, prove by induction a non-recursive upper bound for s_n with limit $\frac{c}{c+\epsilon}$ when $n \rightarrow +\infty$. See formal statement and derivation in §D.2. \square

Prop. 4.2's proof also shows an exponential rate of convergence. Note that if $c \ll \epsilon$ then $\liminf_{n \rightarrow +\infty} \mathbb{P}(f_n \neq \hat{f}_n) \approx 1$. It is reasonable to assume $c \ll \epsilon$ when g has low collision, since c represents the probability of the estimator $\hat{g}(y)$ arriving at the correct output $g(x)$ by chance when given the wrong input $y \neq x$. More details in §D.3.

Moreover, repeated applications of a function often imply unbounded errors: if $g(x)$ can be expressed as an affine transformation $Fx + c$, then it may be viewed as a first-order vector autoregression, which are known to be unstable when $|\lambda| \geq 1$ for at least one λ eigenvalue of F [27] (statement in §D.4). While we make these arguments with affine maps, similar behaviors, perhaps even more acute, would hold with nonlinear maps [22]—but their study is beyond the scope of this paper.

In Prop. 4.2's current form, we implicitly assume that there is a single valid reasoning for each input since g is a function. We can potentially generalize this assumption with a state-transition framing, where the probability of transitioning from a valid state to an invalid one is ϵ , and the probability of recovering from an invalid state is at most c . See formal statement in D.2.

All tasks evaluated in the present work can be seen as instances of the results just proven. Prop. 4.1 directly applies to multiplication, since m -by- n digit multiplication can be seen as n independent instances of m -by-1 digit multiplication (see Cor. D.1). Prop. 4.2 directly applies to the recursive function of the dynamic programming task, as well as to m -by-1 digit multiplication, and to the puzzle through its elimination function (details in D.3). They are also all low collision settings.

5 Discussion

Collapsed Compositionality and Robustness Implications Transformers today demonstrate undeniably powerful empirical results. Yet, our study suggests that Transformers may have fundamental weaknesses in certain intellectual tasks that require true multi-step compositional operations such as multiplications and logic puzzles. Our careful study based on the computation graph and analyses demonstrates that Transformers can often solve multi-step compositional problems by collapsing the depth of the compositional operations via analogical pattern matching. More broadly, our findings suggest that the strong performance of Transformers should be taken with a certain grain of salt: Despite initially appearing challenging, certain tasks may not possess the inherent compositionality they seem to have. This is due to the fact that desired solutions could be readily derived from input-output sequences present in the training data, allowing for shortcut pattern matching to produce acceptable solutions. However, such an approach can ultimately result in poor generalization capabilities as shown in our study. For example, fine-tuning GPT3 on our tasks both with and without explicit reasoning graphs shows that models' learning fails to generalize beyond levels of complexity seen in training.

Theoretical Findings and their Empirical Implications The proofs presented in §4 show that, under reasonable assumptions, the probability of incorrect predictions converges exponentially to ≈ 1 for abstract compositional tasks. Importantly, these proofs apply to autoregressive language models in general. Building on these findings, we suggest several empirical strategies for harnessing the potential of Transformers. Firstly, Transformers may be employed in ways that require chaining only a few compositional steps to reach a solution rather than lengthy reasoning steps (e.g., [30]). Secondly, Transformers may be best suited for compositional tasks where evaluation metrics can afford some leniency; for example, finding approximate solutions that do not require executing the whole graph, such as identifying the most significant digit in a multiplication. Finally, we suggest augmenting Transformers with planning modules as well as using refinement methods, that can iteratively improve their generations [64, 37].

Call for broad Participation to Investigation on the Limitations Identification of limitations is an important step towards achieving greater robustness. Our study suggests fundamental limitations that impede Transformers from fully mastering certain compositional operations. However, we acknowledge that due to our compute budget constraints as well as limited access to the largest language models such as GPT-4, we are unable to push the empirical limits of Transformers even further in terms of training data size and number of epochs. We invite the broader research community, particularly those with more extensive resources at their disposal, to investigate these possibilities further.

6 Related Work

Reasoning abilities in Transformer LLMs Recently, Transformers [9, 42, 41, 14, 13, 46, 56, 57] have demonstrated impressive reasoning abilities across a wide range of tasks, even outperforming humans in certain cases [61, 25, 12, 66]. This success has been largely attributed to the scaling effect, where larger models and training datasets result in improved performance [33, 28, 1]. However, these models have also been shown to struggle across multiple domains, including algorithmic reasoning [60], commonsense reasoning [45, 35], theory of mind [48], planning [59], logical reasoning [53], and ethical reasoning [31]. These difficulties have motivated us to take a step back and thoroughly examine both the successes and failures of Transformers from empirical and theoretical perspectives on compositional reasoning tasks.

Challenges of Transformers in compositional tasks Transformers perform fairly well in single-step reasoning tasks [53], but face challenges when it comes to effectively combining multiple steps to solve compositionally complex problems [39, 49, 63]. Recent research has focused on overcoming these limitations through various approaches. First, fine-tuning Transformers to directly generate the final answer while keeping the reasoning implicit [7, 15]. Second, encouraging Transformers to generate reasoning steps explicitly within a single generation [39, 62, 36]. For example, Nye et al. [39] and Zhou et al. [67] used scratchpads to teach Transformers how to perform algorithmic reasoning tasks such as addition by splitting the task into intermediate steps [36, 62]. Lastly, leveraging LLMs to generate each reasoning step iteratively via a selection and inference mechanism [17, 16, 55]. The primary focus of these studies is to explore possibilities for improving models’ performances on compositional problems without necessarily aiming for complete mastery of the task. While they have indeed made enhancements compared to baseline approaches, they did not achieve 100% accuracy on OOD domain. In contrast, our work delves into investigating the fundamental limits of achieving full mastery of the task. We seek to examine whether we could achieve 100% performance in both in-domain and OOD settings by pushing transformers to their limits. Our findings reveal that accomplishing this feat is not a simple task, and we offer insights into why reaching full mastery is inherently challenging.

Challenges of Transformers in generalization Extensive research has been done to investigate the generalization capabilities of Transformers [3, 38, 23, 47]. This encompasses various facets of generalization, including easy-to-hard generalization [50, 4], length generalization [2, 43, 11, 38], and generalization on symbolic mathematical integration [65]. Schwarzschild et al. [50] and Bansal et al. [4] employ weight-tied neural networks to generalize from easy to hard examples. Razeghi et al. [47] revealed a positive correlation between the frequency of training terms and their test performance. Building upon this line of inquiry, we present a more rigorous examination of sub-graph matching

between training and test instances for complex compositional tasks. We complement our empirical results with theoretical insights on Transformers’ limits.

Iterated Functions The process of repeatedly applying a noisy single operation or function f can be related to iterated random functions [21]. In this latter literature, the focus is usually on the contractive regime in which accrued errors can be kept under control, and the subsequent convergence guarantees (e.g., [20]). When f is an affine transformation, the process falls simultaneously between two perspectives: time series [27] and dynamic programming and control [6]. We leverage the former to discuss the often explosive errors of f^n .

7 Conclusions

On a broader scope, as Transformers continue to gain widespread deployment with significant real-world impacts, it is ever more urgent to understand their successes and failures. Our study critically investigates Transformers’ limitations and emphasizes the need to develop models capable of robust generalization and systematic problem-solving. By examining the compositional capabilities of these models, we aspire to work towards more reliable AI systems that excel not only in tasks where abundant training examples are sufficient, but also in cases requiring precise compositional reasoning.

8 Limitations

We focus on analyzing compositional reasoning capabilities through the lens of computation graphs. Although they are a useful way to systematically represent rigorous reasoning processes, it is important to note that for the scratchpad approach, we are limited to only establishing a correlation between the model generation and its preceding context, as we cannot inspect the exact tokens model attends to when making the prediction. This limitation arises from our lack of access to the activations of the studied models. Furthermore, we posit that alternative approaches to linearizing reasoning processes may yield different performances and provide opportunities for further exploration.

Acknowledgements

We thank members of the Mosaic team at AI2 for valuable feedback on this project, and Agustín Santiago Gutiérrez for valuable discussions. This research was supported by the NSF DMS-2134012, DARPA MCS program through NIWC Pacific (N66001-19-2-4031), and the Allen Institute for AI.

References

- [1] Armen Aghajanyan, Lili Yu, Alexis Conneau, Wei-Ning Hsu, Karen Hambardzumyan, Susan Zhang, Stephen Roller, Naman Goyal, Omer Levy, and Luke Zettlemoyer. Scaling laws for generative mixed-modal language models. *CoRR*, abs/2301.03728, 2023.
- [2] Cem Anil, Yuhuai Wu, Anders Andreassen, Aitor Lewkowycz, Vedant Misra, Vinay Ramasesh, Ambrose Slone, Guy Gur-Ari, Ethan Dyer, and Behnam Neyshabur. Exploring length generalization in large language models. In S. Koyejo, S. Mohamed, A. Agarwal, D. Belgrave, K. Cho, and A. Oh, editors, *Advances in Neural Information Processing Systems*, volume 35, pages 38546–38556. Curran Associates, Inc., 2022.
- [3] Cem Anil, Yuhuai Wu, Anders Johan Andreassen, Aitor Lewkowycz, Vedant Misra, Vinay Venkatesh Ramasesh, Ambrose Slone, Guy Gur-Ari, Ethan Dyer, and Behnam Neyshabur. Exploring length generalization in large language models. In *Advances in Neural Information Processing Systems*, volume 35, pages 38546–38556. Curran Associates, Inc., 2022.
- [4] Arpit Bansal, Avi Schwarzschild, Eitan Borgnia, Zeyad Emam, Furong Huang, Micah Goldblum, and Tom Goldstein. End-to-end algorithm synthesis with recurrent networks: Extrapolation without overthinking. In S. Koyejo, S. Mohamed, A. Agarwal, D. Belgrave, K. Cho, and A. Oh, editors, *Advances in Neural Information Processing Systems*, volume 35, pages 20232–20242. Curran Associates, Inc., 2022.
- [5] Yoshua Bengio, Réjean Ducharme, and Pascal Vincent. A neural probabilistic language model. In *Advances in Neural Information Processing Systems*, volume 13. MIT Press, 2000.
- [6] D. Bertsekas. *Abstract Dynamic Programming: 3rd Edition*. Athena scientific optimization and computation series. Athena Scientific., 2022.
- [7] Gregor Betz, Christian Voigt, and Kyle Richardson. Critical thinking for language models. In *Proceedings of the 14th International Conference on Computational Semantics (IWCS)*, pages 63–75, 2021.
- [8] Ning Bian, Xianpei Han, Le Sun, Hongyu Lin, Yaojie Lu, and Ben He. ChatGPT is a knowledgeable but inexperienced solver: An investigation of commonsense problem in large language models. *CoRR*, abs/2303.16421, 2023.
- [9] Tom Brown, Benjamin Mann, Nick Ryder, Melanie Subbiah, Jared D. Kaplan, Prafulla Dhariwal, Arvind Neelakantan, Pranav Shyam, Girish Sastry, Amanda Askell, Sandhini Agarwal, Ariel Herbert-Voss, Gretchen Krueger, Tom Henighan, Rewon Child, Aditya Ramesh, Daniel Ziegler, Jeffrey Wu, Clemens Winter, Chris Hesse, Mark Chen, Eric Sigler, Mateusz Litwin, Scott Gray, Benjamin Chess, Jack Clark, Christopher Berner, Sam McCandlish, Alec Radford, Ilya Sutskever, and Dario Amodei. Language models are few-shot learners. In *Advances in Neural Information Processing Systems*, volume 33, pages 1877–1901, 2020.
- [10] Sébastien Bubeck, Varun Chandrasekaran, Ronen Eldan, Johannes Gehrke, Eric Horvitz, Ece Kamar, Peter Lee, Yin Tat Lee, Yuanzhi Li, Scott M. Lundberg, Harsha Nori, Hamid Palangi, Marco Túlio Ribeiro, and Yi Zhang. Sparks of artificial general intelligence: Early experiments with GPT-4. *CoRR*, abs/2303.12712, 2023.
- [11] Mirelle Bueno, Carlos Gemmel, Jeffrey Dalton, Roberto de Alencar Lotufo, and Rodrigo Frassetto Nogueira. Induced natural language rationales and interleaved markup tokens enable extrapolation in large language models. *CoRR*, abs/2208.11445, 2022.
- [12] Jonathan H Choi, Kristin E Hickman, Amy Monahan, and Daniel Schwarcz. ChatGPT goes to law school. *Available at SSRN*, 2023.
- [13] Aakanksha Chowdhery, Sharan Narang, Jacob Devlin, Maarten Bosma, Gaurav Mishra, Adam Roberts, Paul Barham, Hyung Won Chung, Charles Sutton, Sebastian Gehrmann, Parker Schuh, Kensen Shi, Sasha Tsvyashchenko, Joshua Maynez, Abhishek Rao, Parker Barnes, Yi Tay, Noam Shazeer, Vinodkumar Prabhakaran, Emily Reif, Nan Du, Ben Hutchinson, Reiner Pope, James Bradbury, Jacob Austin, Michael Isard, Guy Gur-Ari, Pengcheng Yin,

- Toju Duke, Anselm Levskaya, Sanjay Ghemawat, Sunipa Dev, Henryk Michalewski, Xavier Garcia, Vedant Misra, Kevin Robinson, Liam Fedus, Denny Zhou, Daphne Ippolito, David Luan, Hyeontaek Lim, Barret Zoph, Alexander Spiridonov, Ryan Sepassi, David Dohan, Shivani Agrawal, Mark Omernick, Andrew M. Dai, Thanumalayan Sankaranarayana Pillai, Marie Pellat, Aitor Lewkowycz, Erica Moreira, Rewon Child, Oleksandr Polozov, Katherine Lee, Zongwei Zhou, Xuezhi Wang, Brennan Saeta, Mark Diaz, Orhan Firat, Michele Catasta, Jason Wei, Kathy Meier-Hellstern, Douglas Eck, Jeff Dean, Slav Petrov, and Noah Fiedel. Palm: Scaling language modeling with pathways. *CoRR*, abs/2204.02311, 2022.
- [14] Hyung Won Chung, Le Hou, Shayne Longpre, Barret Zoph, Yi Tay, William Fedus, Eric Li, Xuezhi Wang, Mostafa Dehghani, Siddhartha Brahma, Albert Webson, Shixiang Shane Gu, Zhuyun Dai, Mirac Suzgun, Xinyun Chen, Aakanksha Chowdhery, Sharan Narang, Gaurav Mishra, Adams Yu, Vincent Y. Zhao, Yanping Huang, Andrew M. Dai, Hongkun Yu, Slav Petrov, Ed H. Chi, Jeff Dean, Jacob Devlin, Adam Roberts, Denny Zhou, Quoc V. Le, and Jason Wei. Scaling instruction-finetuned language models. *CoRR*, abs/2210.11416, 2022.
 - [15] Peter Clark, Oyvind Tafjord, and Kyle Richardson. Transformers as soft reasoners over language. In *Proceedings of the Twenty-Ninth International Conference on International Joint Conferences on Artificial Intelligence*, pages 3882–3890, 2021.
 - [16] Antonia Creswell and Murray Shanahan. Faithful reasoning using large language models. *CoRR*, abs/2208.14271, 2022.
 - [17] Antonia Creswell, Murray Shanahan, and Irina Higgins. Selection-inference: Exploiting large language models for interpretable logical reasoning. In *International Conference on Learning Representations*, 2023.
 - [18] Leonardo De Moura and Nikolaj Bjørner. Z3: An efficient smt solver. In *Tools and Algorithms for the Construction and Analysis of Systems: 14th International Conference, TACAS 2008, Held as Part of the Joint European Conferences on Theory and Practice of Software, ETAPS 2008, Budapest, Hungary, March 29-April 6, 2008. Proceedings 14*, pages 337–340. Springer, 2008.
 - [19] Stanislas Dehaene, Nicolas Molko, Laurent Cohen, and Anna J Wilson. Arithmetic and the brain. *Current opinion in neurobiology*, 14(2):218–224, 2004.
 - [20] B. Delyon and A. Juditsky. On small perturbations of stable markov operators: Unbounded case. *Theory of Probability & Its Applications*, 43(4):577–587, 1999.
 - [21] Persi Diaconis and David Freedman. Iterated random functions. *SIAM review*, 41(1):45–76, 1999.
 - [22] R. Douc, E. Moulines, and D. Stoffer. *Nonlinear Time Series: Theory, Methods and Applications with R Examples*. Chapman & Hall/CRC Texts in Statistical Science. Taylor & Francis, 2014.
 - [23] Yann Dubois, Gautier Dagan, Dieuwke Hupkes, and Elia Bruni. Location attention for extrapolation to longer sequences. In *Proceedings of the 58th Annual Meeting of the Association for Computational Linguistics*, pages 403–413, 2020.
 - [24] Jonathan St BT Evans. *Bias in human reasoning: Causes and consequences*. Lawrence Erlbaum Associates, Inc, 1989.
 - [25] Hao Fu, Yao; Peng and Tushar Khot. How does gpt obtain its ability? tracing emergent abilities of language models to their sources. *Yao Fu's Notion*, Dec 2022.
 - [26] Robert Geirhos, Jörn-Henrik Jacobsen, Claudio Michaelis, Richard Zemel, Wieland Brendel, Matthias Bethge, and Felix A Wichmann. Shortcut learning in deep neural networks. *Nature Machine Intelligence*, 2(11):665–673, 2020.
 - [27] James Douglas Hamilton. *Time series analysis*. Princeton university press, 1994.

- [28] Tom Henighan, Jared Kaplan, Mor Katz, Mark Chen, Christopher Hesse, Jacob Jackson, Heewoo Jun, Tom B. Brown, Prafulla Dhariwal, Scott Gray, Chris Hallacy, Benjamin Mann, Alec Radford, Aditya Ramesh, Nick Ryder, Daniel M. Ziegler, John Schulman, Dario Amodei, and Sam McCandlish. Scaling laws for autoregressive generative modeling. *CoRR*, abs/2010.14701, 2020.
- [29] James Hiebert. *Conceptual and procedural knowledge: The case of mathematics*. Routledge, 2013.
- [30] Albert Qiaochu Jiang, Sean Welleck, Jin Peng Zhou, Timothee Lacroix, Jiacheng Liu, Wenda Li, Mateja Jamnik, Guillaume Lample, and Yuhuai Wu. Draft, sketch, and prove: Guiding formal theorem provers with informal proofs. In *The Eleventh International Conference on Learning Representations*, 2023.
- [31] Liwei Jiang, Jena D. Hwang, Chandra Bhagavatula, Ronan Le Bras, Maxwell Forbes, Jon Borchardt, Jenny Liang, Oren Etzioni, Maarten Sap, and Yejin Choi. Delphi: Towards machine ethics and norms. *CoRR*, abs/2110.07574, 2021.
- [32] Philip N Johnson-Laird, Sangeet S Khemlani, and Geoffrey P Goodwin. Logic, probability, and human reasoning. *Trends in cognitive sciences*, 19(4):201–214, 2015.
- [33] Jared Kaplan, Sam McCandlish, Tom Henighan, Tom B. Brown, Benjamin Chess, Rewon Child, Scott Gray, Alec Radford, Jeffrey Wu, and Dario Amodei. Scaling laws for neural language models. *CoRR*, abs/2001.08361, 2020.
- [34] Jon Kleinberg and Eva Tardos. *Algorithm Design*. Addison-Wesley Longman Publishing Co., Inc., USA, 2005.
- [35] Philipp E. Koralus and Vincent Wang-Mascianica. Humans in humans out: On GPT converging toward common sense in both success and failure. *CoRR*, abs/2303.17276, 2023.
- [36] Wang Ling, Dani Yogatama, Chris Dyer, and Phil Blunsom. Program induction by rationale generation: Learning to solve and explain algebraic word problems. In *Proceedings of the 55th Annual Meeting of the Association for Computational Linguistics (Volume 1: Long Papers)*, pages 158–167, 2017.
- [37] Aman Madaan, Niket Tandon, Prakhar Gupta, Skyler Hallinan, Luyu Gao, Sarah Wiegreffe, Uri Alon, Nouha Dziri, Shrimai Prabhumoye, Yiming Yang, Sean Welleck, Bodhisattwa Prasad Majumder, Shashank Gupta, Amir Yazdanbakhsh, and Peter Clark. Self-refine: Iterative refinement with self-feedback. *CoRR*, abs/2303.17651, 2023.
- [38] Benjamin Newman, John Hewitt, Percy Liang, and Christopher D Manning. The eos decision and length extrapolation. In *Proceedings of the Third BlackboxNLP Workshop on Analyzing and Interpreting Neural Networks for NLP*, pages 276–291, 2020.
- [39] Maxwell Nye, Anders Johan Andreassen, Guy Gur-Ari, Henryk Michalewski, Jacob Austin, David Bieber, David Dohan, Aitor Lewkowycz, Maarten Bosma, David Luan, Charles Sutton, and Augustus Odena. Show your work: Scratchpads for intermediate computation with language models, 2021.
- [40] Maxwell I. Nye, Anders Johan Andreassen, Guy Gur-Ari, Henryk Michalewski, Jacob Austin, David Bieber, David Dohan, Aitor Lewkowycz, Maarten Bosma, David Luan, Charles Sutton, and Augustus Odena. Show your work: Scratchpads for intermediate computation with language models. *CoRR*, abs/2112.00114, 2021.
- [41] OpenAI. ChatGPT: Optimizing language models for dialogue, 2022.
- [42] OpenAI. GPT-4 technical report, 2023.
- [43] Ofir Press, Noah Smith, and Mike Lewis. Train short, test long: Attention with linear biases enables input length extrapolation. In *International Conference on Learning Representations*, 2022.

- [44] Patrick Prosser. Hybrid algorithms for the constraint satisfaction problem. *Computational intelligence*, 9(3):268–299, 1993.
- [45] Chengwei Qin, Aston Zhang, Zhuosheng Zhang, Jiaao Chen, Michihiro Yasunaga, and Diyi Yang. Is ChatGPT a general-purpose natural language processing task solver? *CoRR*, abs/2302.06476, 2023.
- [46] Jack W. Rae, Sebastian Borgeaud, Trevor Cai, Katie Millican, Jordan Hoffmann, Francis Song, John Aslanides, Sarah Henderson, Roman Ring, Susannah Young, Eliza Rutherford, Tom Hennigan, Jacob Menick, Albin Cassirer, Richard Powell, George van den Driessche, Lisa Anne Hendricks, Maribeth Rauh, Po-Sen Huang, Amelia Glaese, Johannes Welbl, Sumanth Dathathri, Saffron Huang, Jonathan Uesato, John F. J. Mellor, Irina Higgins, Antonia Creswell, Nathan McAleese, Amy Wu, Erich Elsen, Siddhant M. Jayakumar, Elena Buchatskaya, David Budden, Esme Sutherland, Karen Simonyan, Michela Paganini, L. Sifre, Lena Martens, Xiang Lorraine Li, Adhiguna Kuncoro, Aida Nematzadeh, Elena Gribovskaya, Domenic Donato, Angeliki Lazaridou, Arthur Mensch, Jean-Baptiste Lespiau, Maria Tsimpoukelli, N. K. Grigorev, Doug Fritz, Thibault Sottiaux, Mantas Pajarskas, Tobias Pohlen, Zhitao Gong, Daniel Toyama, Cyprien de Masson d’Autume, Yujia Li, Tayfun Terzi, Vladimir Mikulik, Igor Babuschkin, Aidan Clark, Diego de Las Casas, Aurelia Guy, Chris Jones, James Bradbury, Matthew G. Johnson, Blake A. Hechtman, Laura Weidinger, Jason Gabriel, William S. Isaac, Edward Lockhart, Simon Osindero, Laura Rimell, Chris Dyer, Oriol Vinyals, Kareem W. Ayoub, Jeff Stanway, L. L. Bennett, Demis Hassabis, Koray Kavukcuoglu, and Geoffrey Irving. Scaling language models: Methods, analysis & insights from training gopher. *ArXiv*, abs/2112.11446, 2021.
- [47] Yasaman Razeghi, Robert L Logan IV, Matt Gardner, and Sameer Singh. Impact of pretraining term frequencies on few-shot numerical reasoning. In *Findings of the Association for Computational Linguistics: EMNLP 2022*, pages 840–854, Abu Dhabi, United Arab Emirates, December 2022. Association for Computational Linguistics.
- [48] Maarten Sap, Ronan Le Bras, Daniel Fried, and Yejin Choi. Neural theory-of-mind? on the limits of social intelligence in large LMs. In *Proceedings of the 2022 Conference on Empirical Methods in Natural Language Processing*, pages 3762–3780, Abu Dhabi, United Arab Emirates, December 2022. Association for Computational Linguistics.
- [49] Abulhair Saparov and He He. Language models are greedy reasoners: A systematic formal analysis of chain-of-thought. In *International Conference on Learning Representations*, 2023.
- [50] Avi Schwarzschild, Eitan Borgnia, Arjun Gupta, Furong Huang, Uzi Vishkin, Micah Goldblum, and Tom Goldstein. Can you learn an algorithm? generalizing from easy to hard problems with recurrent networks. In *Advances in Neural Information Processing Systems*, volume 34, pages 6695–6706. Curran Associates, Inc., 2021.
- [51] Herbert A. Simon. The architecture of complexity. *Proceedings of the American Philosophical Society*, 106(6):467–482, 1962.
- [52] Herbert A Simon and Allen Newell. Human problem solving: The state of the theory in 1970. *American Psychologist*, 26(2):145, 1971.
- [53] Aarohi Srivastava, Abhinav Rastogi, Abhishek Rao, Abu Awal Md Shoeb, Abubakar Abid, Adam Fisch, Adam R. Brown, Adam Santoro, Aditya Gupta, Adrià Garriga-Alonso, Agnieszka Kluska, Aitor Lewkowycz, Akshat Agarwal, Alethea Power, Alex Ray, Alex Warstadt, Alexander W. Kocurek, Ali Safaya, Ali Tazarv, Alice Xiang, Alicia Parrish, Allen Nie, Aman Hussain, Amanda Askell, Amanda Dsouza, Ameet Rahane, Anantharaman S. Iyer, Anders Andreassen, Andrea Santilli, Andreas Stuhlmüller, Andrew M. Dai, Andrew La, Andrew K. Lampinen, Andy Zou, Angela Jiang, Angelica Chen, Anh Vuong, Animesh Gupta, Anna Gottardi, Antonio Norelli, Anu Venkatesh, Arash Gholamidavoodi, Arfa Tabassum, Arul Menezes, Arun Kirubarajan, Asher Mullokandov, Ashish Sabharwal, Austin Herrick, Avia Efrat, Aykut Erdem, Ayla Karakas, and et al. Beyond the imitation game: Quantifying and extrapolating the capabilities of language models. *CoRR*, abs/2206.04615, 2022.
- [54] Keith Stenning and Michiel Van Lambalgen. *Human reasoning and cognitive science*. MIT Press, 2012.

- [55] Oyvind Tafjord, Bhavana Dalvi, and Peter Clark. Proofwriter: Generating implications, proofs, and abductive statements over natural language. In *Findings of the Association for Computational Linguistics: ACL-IJCNLP 2021*, pages 3621–3634, 2021.
- [56] Ross Taylor, Marcin Kardas, Guillem Cucurull, Thomas Scialom, Anthony Hartshorn, Elvis Saravia, Andrew Poulton, Viktor Kerkez, and Robert Stojnic. Galactica: A large language model for science. *CoRR*, abs/2211.09085, 2022.
- [57] Romal Thoppilan, Daniel De Freitas, Jamie Hall, Noam Shazeer, Apoorv Kulshreshtha, Heng-Tze Cheng, Alicia Jin, Taylor Bos, Leslie Baker, Yu Du, YaGuang Li, Hongrae Lee, Huaixiu Steven Zheng, Amin Ghafouri, Marcelo Menegali, Yanping Huang, Maxim Krikun, Dmitry Lepikhin, James Qin, Dehao Chen, Yuanzhong Xu, Zhifeng Chen, Adam Roberts, Maarten Bosma, Yanqi Zhou, Chung-Ching Chang, Igor Krivokon, Will Rusch, Marc Pickett, Kathleen S. Meier-Hellstern, Meredith Ringel Morris, Tulsee Doshi, Renelito Delos Santos, Toju Duke, Johnny Soraker, Ben Zevenbergen, Vinodkumar Prabhakaran, Mark Diaz, Ben Hutchinson, Kristen Olson, Alejandra Molina, Erin Hoffman-John, Josh Lee, Lora Aroyo, Ravi Rajakumar, Alena Butryna, Matthew Lamm, Viktoriya Kuzmina, Joe Fenton, Aaron Cohen, Rachel Bernstein, Ray Kurzweil, Blaise Aguera-Arcas, Claire Cui, Marian Croak, Ed H. Chi, and Quoc Le. Lamda: Language models for dialog applications. *CoRR*, abs/2201.08239, 2022.
- [58] Hugo Touvron, Thibaut Lavril, Gautier Izacard, Xavier Martinet, Marie-Anne Lachaux, Timothée Lacroix, Baptiste Rozière, Naman Goyal, Eric Hambro, Faisal Azhar, Aurélien Rodriguez, Armand Joulin, Edouard Grave, and Guillaume Lample. LLaMA: Open and efficient foundation language models. *CoRR*, abs/2302.13971, 2023.
- [59] Karthik Valmeekam, Alberto Olmo, Sarath Sreedharan, and Subbarao Kambhampati. Large language models still can't plan (a benchmark for LLMs on planning and reasoning about change). In *NeurIPS 2022 Foundation Models for Decision Making Workshop*, 2022.
- [60] Petar Veličković and Charles Blundell. Neural algorithmic reasoning. *Patterns*, 2(7):100273, 2021.
- [61] Jason Wei, Yi Tay, Rishi Bommasani, Colin Raffel, Barret Zoph, Sebastian Borgeaud, Dani Yogatama, Maarten Bosma, Denny Zhou, Donald Metzler, Ed H. Chi, Tatsunori Hashimoto, Oriol Vinyals, Percy Liang, Jeff Dean, and William Fedus. Emergent abilities of large language models. *Transactions on Machine Learning Research*, 2022. Survey Certification.
- [62] Jason Wei, Xuezhi Wang, Dale Schuurmans, Maarten Bosma, brian ichter, Fei Xia, Ed Chi, Quoc V Le, and Denny Zhou. Chain-of-thought prompting elicits reasoning in large language models. In *Advances in Neural Information Processing Systems*, volume 35, pages 24824–24837. Curran Associates, Inc., 2022.
- [63] Sean Welleck, Jiacheng Liu, Ximing Lu, Hannaneh Hajishirzi, and Yejin Choi. NaturalProver: Grounded mathematical proof generation with language models. In *Advances in Neural Information Processing Systems*, volume 35, pages 4913–4927. Curran Associates, Inc., 2022.
- [64] Sean Welleck, Ximing Lu, Peter West, Faeze Brahman, Tianxiao Shen, Daniel Khashabi, and Yejin Choi. Generating sequences by learning to self-correct. In *International Conference on Learning Representations*, 2023.
- [65] Sean Welleck, Peter West, Jize Cao, and Yejin Choi. Symbolic brittleness in sequence models: on systematic generalization in symbolic mathematics. In *Proceedings of the AAAI Conference on Artificial Intelligence*, volume 36, pages 8629–8637, 2022.
- [66] Haoyi Zheng and Huichun Zhan. ChatGPT in scientific writing: a cautionary tale. *The American Journal of Medicine*, 2023.
- [67] Hattie Zhou, Azade Nova, Aaron Courville, Hugo Larochelle, Behnam Neyshabur, and Hanie Sedghi. Teaching algorithmic reasoning via in-context learning, 2023.

Appendices

A Compositional Tasks	17
A.1 Multiplication	17
A.2 Einstein’s Puzzle	18
A.3 Dynamic Programming Problem	20
B Experimental Setups & Empirical Results	22
B.1 Models	22
B.2 Limits of Transformers in Zero- and Few-shot Settings	22
B.3 Limits of Transformers with question-answer Training	22
B.4 Limits of Transformers with Explicit Scratchpad Training	23
C Surface Patterns	26
C.1 Relative Information Gain Predictions for Multiplication	26
C.2 Empirical Surface Pattern Analysis for Multiplication with GPT4, ChatGPT and GPT3	27
C.3 Relative Information Gain Predictions for Dynamic Programming Task	28
C.4 Empirical Surface Pattern Results for Dynamic Programming Task	30
D Theoretical Results: Derivations	32
D.1 Transformers struggle with problems with increasingly larger parallelism (<i>width</i>) .	32
D.2 Transformers struggle with problems that require increasingly larger iterative applications of a function (<i>depth</i>)	33
D.3 Discussing $c \ll \epsilon$ in the context of Proposition 4.2	35
D.4 Error rates in repeated applications of a function may be unbounded	36
E Societal impact	37

A Compositional Tasks

A.1 Multiplication

Data Construction We exhaustively generate multiplication problems as question-answer pairs (e.g., Q: “What is 4 times 32?” A: “128”). We focus on multiplications of two numbers $x = (x_1, x_2, \dots, x_k)$ and $y = (y_1, y_2, \dots, y_k)$ where each number can have up to k digits, amounting to $9 \times 10^{(k-1)}$ combinations per each number. We set k to 5 in our experiments. Figure 7 showcases an example prompt for performing few-shot learning without the inclusion of a scratchpad, while Figure 8 demonstrates an example prompt using a scratchpad. Throughout our experimentation, we explored various versions of the scratchpad, ranging from verbose and detailed to more concise alternatives. Among these variations, the scratchpad version depicted in Figure 8 ultimately produced the most favorable outcomes. Listing 1 shows the Python code for solving the task.

To multiply two numbers, start by multiplying the rightmost digit of the multiplicand by each digit of the multiplier, writing down the products and carrying over any remainders. Repeat this process for each digit of the multiplicand, and then add up all the partial products to obtain the final result.

Questions: what's 22 times 2? Answer 44.

Figure 7: Example prompt for the multiplication task used for the few-shot setting.

Question: What is 35 times 90?

Scratchpad: Let's perform the multiplication step by step:

Let's multiply 35 by the digit in the ones place of 90, which is 0.

1. Multiply 0 by the digit in the ones place of 35, which is 5. This gives $5 \times 0 = 0$. Write down the result 0.
2. Multiply 0 by the digit in the tens place of 35, which is 3. This gives $3 \times 0 = 0$. Write down the result 0.
3. The partial product for this step is A=0 which is the concatenation of the digits we found in each step.

Now, let's multiply 35 by the digit in the tens place of 90, which is 9.
Multiply 9 by the digit in the ones place of 35, which is 5. This gives $5 \times 9 = 45$. Write down the result 5 and carry over the 4 to the next step.

5. Multiply 9 by the digit in the tens place of 35, which is 3. Add the carryover from the previous step to account for this. This gives $(3 \times 9) + 4 = 31$. Write down the result 31.
6. The partial product for this step is B=315 which is the concatenation of the digits we found in each step.

Now, let's sum the 2 partial products A and B, and take into account the position of each digit: A=0 (from multiplication by 0) and B=315 (from multiplication by 9 but shifted one place to the left, so it becomes 3150). The final answer is $0 \times 1 + 315 \times 10 = 0 + 3150 = 3150$.

Figure 8: A sample scratchpad for the multiplication task.

```
1 def multiply(x, y):  
2     summands = [0] * len(y)  
3     for i in range(len(y) - 1, -1, -1):
```

```

4     digits = [0] * len(x)
5     carry = 0
6     for j in range(len(x) - 1, -1, -1):
7         t = x[j] * y[i]
8         t += carry
9         carry = t // 10
10        digits[j] = t %
11    digits.insert(0, carry)
12    summands[i] = sum(digits[-k] * (10 ** (k - 1)) for k in range
13    (1, len(digits) + 1))
14
15    product = sum(summands[-i] * (10 ** (i - 1)) for i in range(1, len
(y) + 1))
16    return product

```

Listing 1: Example Python code for solving the multiplication task.

A.2 Einstein's Puzzle

Data Construction In our experiments, we initially establish a set of properties, such as Color, PhoneModel, Pet, and so forth, along with their corresponding values expressed in natural language templates (e.g., “The house has a red color.”). We then devise a fundamental and straightforward set of clue types: 1) ‘found_at’, e.g., “Alice lives in House 2”, 2) ‘same_house’, e.g., “The person who is a cat lover lives in the house that has a red color.”, 3) ‘direct_left’, e.g., “The person who has a dog as a pet lives to the left of the person who lives in a red house.”, and 4) ‘besides’, e.g., “The person who has a dog as a pet and the person who has a red house live next to each other.” In addition, we also set up harder clue types such as ‘not_at’, ‘left_of’ (not necessarily directly left of), ‘two_house_between’, etc. which are only used in auxiliary experiments.

The solution to the puzzle is a matrix of size $K \times M$, where K represents the number of houses and M the number of attributes. During the puzzle generation, the M properties are randomly selected from the candidate pool, followed by the random sampling of K values for each property. The sampled values are then randomly permuted and assigned within the table to create the solution. It is important to note that we ensure one of the sampled properties is ‘Name’ to enhance the readability and comprehensibility of the puzzles. To construct the clues, we initially over-generate all valid clues based on the solution and subsequently remove redundant clues at random until we obtain a set with a

General Unique Rules

There are 3 houses (numbered 1 on the left, 3 on the right). Each has a different person in them. They have different characteristics:

- Each person has a unique **name**: peter, eric, arnold
- People have different favorite **sports**: soccer, tennis, basketball
- People own different **car models**: tesla, ford, camry

Ground-Truth Table

House	Name	Sports	Car
1	Eric	Basketball	Camry
2	Peter	Tennis	Ford
3	Arnold	Soccer	Tesla

Clues

1. The person who owns a **Ford** is the person who loves **tennis**.
2. **Arnold** is in the third house.
3. The person who owns a **Camry** is directly left of the person who owns a **Ford**.
4. **Eric** is the person who owns a **Camry**.
5. The person who loves **basketball** is **Eric**.
6. The person who loves **tennis** and the person who loves **soccer** are next to each other.

Reasoning Path Generation

```

Algorithm 1 Puzzle Solver
Input: Clues
Output: Reasoning path
1: function PUZZLESOLVER(Clues)
2:   Path ← []
3:   LeftClues ← clues
4:   while |LeftClues| ≠ 0 do
5:     for i=1 to |LeftClues| do
6:       CandidateClues = {LeftClues[i]}
7:       for clue in CandidateClues do
8:         if solve any cell then
9:           LeftClues.remove(clue)
10:          Path.append(clue)
11:  return Path

```



Figure 9: A sample of the puzzle task and the reasoning path to reach a solution.

This is a logic puzzle. There are 3 houses (numbered 1 on the left, 3 on the right). Each has a different person in them. They have different characteristics:

- Each person has a unique name: peter, eric, arnold
- People have different favorite sports: soccer, tennis, basketball
- People own different car models: tesla model 3, ford f150, toyota camry

1. The person who owns a Ford F-150 is the person who loves tennis.
2. Arnold is in the third house.
3. The person who owns a Toyota Camry is directly left of the person who owns a Ford F-150.
4. Eric is the person who owns a Toyota Camry.
5. The person who loves basketball is Eric.
6. The person who loves tennis and the person who loves soccer are next to each other.

Let's think step by step. Please first briefly talk about your reasoning and show your final solution by filling the blanks in the below table.

```
$ House: ___ $ Name: ___ $ Sports: ___ $ Car: ___
$ House: ___ $ Name: ___ $ Sports: ___ $ Car: ___
$ House: ___ $ Name: ___ $ Sports: ___ $ Car: ___
```

Reasoning:

Step 1: First apply clue <Arnold is in the third house.> We know that The Name in house 3 is arnold.

Step 2: Then combine clues: <The person who loves tennis and the person who loves soccer are next to each other.> <The person who loves basketball is Eric.> Unique Values Rules and the fixed table structure. We know that The Name in house 1 is eric. The FavoriteSport in house 1 is basketball. The Name in house 2 is peter.

Step 3: Then apply clue <Eric is the person who owns a Toyota Camry.> We know that The CarModel in house 1 is toyota camry.

Step 4: Then apply clue <The person who owns a Toyota Camry is directly left of the person who owns a Ford F-150.> and Unique Values We know that The CarModel in house 2 is ford f150. The CarModel in house 3 is tesla model 3.

Step 5: Then apply clue <The person who owns a Ford F-150 is the person who loves tennis.> and Unique Values We know that The FavoriteSport in house 2 is tennis. The FavoriteSport in house 3 is soccer.

The puzzle is solved.

Final solution:

```
$ House: 1 $ Name: Eric   $ Sports: Basketball $ Car: Camry
$ House: 2 $ Name: Peter   $ Sports: Tennis      $ Car: Ford
$ House: 3 $ Name: Arnold  $ Sports: Soccer     $ Car: Tesla
```

Figure 10: A sample scratchpad for the puzzle task.

unique solution, as previously sampled. This process ensures a coherent and engaging puzzle-solving experience. Refer to Figure 9 for an example.

Graph Construction Algorithm To solve the complex compositional reasoning process for a logical grid puzzle, we use existing puzzle solvers [18] to generate the computation graph. It follows the basic greedy principle of applying the minimum number of rules to solve any cell, i.e., if using only one rule to solve any given cell, then apply this rule. This algorithm iterates through all clues in the clue set until one or a set of clue combinations can solve any cell in the table. While it may not be the most efficient way to solve the puzzle, it provides models with explicit scratchpad verbalization through an intuitive computation graph. Refer to Figure 9 for the pseudo-code of the process, and Figure 10 for a scratchpad example.

A.3 Dynamic Programming Problem

A.3.1 Solution to this problem

Let $a = [a_1, \dots, a_n]$ be an input. Let dp_i be the maximum sum of a subsequence that does not include adjacent elements, when considering only the elements of the input from the i -th position onwards.

Trivially, $dp_n = \max(a_n, 0)$ since we only want to choose a number if it is non-negative. Moreover, $dp_{n-1} = \max(a_n, a_{n-1}, 0)$ since we cannot choose adjacent numbers.

For any given dp_i with $i \leq n - 2$, we can express it in terms of dp_{i+1} and dp_{i+2} . Concretely, the maximum sum of a subsequence starting at position i may or may not include the element in the i -th position, a_i . If the subsequence includes a_i , then the maximum sum is $a_i + dp_{i+2}$, since using a_i blocks us from using the next element. If the subsequence does not include a_i , then its sum is dp_{i+1} . Moreover, the answer may never be less than zero, because otherwise we would select the empty sequence⁵. In summary,

$$dp_i = \max(dp_{i+1}, a_i + dp_{i+2}, 0)$$

We now have a recursion with its base cases $dp_n = \max(a_n, 0)$ and $dp_{n-1} = \max(a_n, a_{n-1}, 0)$, and we can therefore compute all values in $O(n)$. It now only rests to reconstruct the lexicographically smallest subsequence that maximizes the desired sum, based solely on the computed dp values.

Starting from dp_1 and iterating sequentially through dp_{n-2} , we choose an item if and only if $dp_i = a_i + dp_{i+2}$ (that is, the maximum sum comes from choosing the current element) and we have not chosen the previous element. This helps disambiguate cases where choosing or not choosing a_i yields the same sum, but possibly only one of those will not incur in choosing adjacent numbers. Similarly, for positions $i = n - 1$ and $i = n$ we choose the element if $dp_i = a_i$ (that is, choosing the element yields the maximum sum) and we have not chosen the immediately previous element. See an example Python solution in 2.

Given a sequence of integers, find a subsequence with the highest sum, such that no two numbers in the subsequence are adjacent in the original sequence.

Output a list with "1" for chosen numbers and "2" for unchosen ones. If multiple solutions exist, select the lexicographically smallest. input = [3, 2, 1, 5, 2].

Figure 11: Example prompt for the DP task, used for zero-shot and few-shot settings.

```

1 def maximum_sum_nonadjacent_subsequence(arr):
2
3     N = len(arr)
4     dp = [0 for _ in range(N)]
5
6     dp[N - 1] = max(arr[N - 1], 0)
7     dp[N - 2] = max(max(arr[N - 1], arr[N - 2]), 0)
8
9     for i in range(N - 3, -1, -1):
10         dp[i] = max(max(dp[i + 1], arr[i] + dp[i + 2]), 0)
11
12     # reconstruct the answer with a fixed-size graph
13     result = []
14     can_use_next_item = True
15
16     for i in range(N - 2):
17         if dp[i] == arr[i] + dp[i + 2] and can_use_next_item:
18             result.append(1)
19             can_use_next_item = False
20         else:

```

⁵We don't need to explicitly check for this since $dp_n \geq 0$. However, we include the condition to ease the scratchpad logic.

```

21     result.append(2)
22     can_use_next_item = True
23
24     if dp[N - 2] == arr[N - 2] and can_use_next_item:
25         result.append(1)
26         can_use_next_item = False
27     else:
28         result.append(2)
29         can_use_next_item = True
30
31     if dp[N - 1] == arr[N - 1] and can_use_next_item:
32         result.append(1)
33     else:
34         result.append(2)
35
36 return result

```

Listing 2: Example Python code for solving the DP task. We chose this implementation because the computation graph has always the same topology for any given input length.

Question: Let's solve input = [3, 2, 1, 5, 2].

```

Scratchpad: dp[4] = max(input[4], 0) = max(2, 0) = 2
dp[3] = max(input[3], input[4], 0) = max(5, 2, 0) = 5
dp[2] = max(dp[3], input[2] + dp[4], 0) = max(5, 1 + 2, 0) = 5
dp[1] = max(dp[2], input[1] + dp[3], 0) = max(5, 2 + 5, 0) = 7
dp[0] = max(dp[1], input[0] + dp[2], 0) = max(7, 3 + 5, 0) = 8

```

Finally, we reconstruct the lexicographically smallest subsequence that fulfills the task objective by selecting numbers as follows. We store the result on a list named "output".

Let can_use_next_item = True.
Since $dp[0] == input[0] + dp[2]$ ($8 == 3 + 5$) and $can_use_next_item == True$, we store $output[0] = 1$. We update $can_use_next_item = False$.
Since $dp[1] != input[1] + dp[3]$ ($7 != 2 + 5$) or $can_use_next_item == False$, we store $output[1] = 2$. We update $can_use_next_item = True$.
Since $dp[2] != input[2] + dp[4]$ ($5 != 1 + 2$) or $can_use_next_item == False$, we store $output[2] = 2$. We update $can_use_next_item = True$.
Since $dp[3] == input[3]$ ($5 == 5$) and $can_use_next_item == True$, we store $output[3] = 1$. We update $can_use_next_item = False$.
Since $dp[4] != input[4]$ ($2 != 2$) or $can_use_next_item == False$, we store $output[4] = 2$.

Reconstructing all together, output=[1, 2, 2, 1, 2].

Figure 12: A sample scratchpad for the DP task used for fine-tuning with few-shot settings.

Data Construction We exhaustively generate data for this DP task. For question-answer setting, we include a thorough explanation of the task before asking to generate a solution (see Figure 11). We use all lists up to 5 elements as training, and we consider only lists where elements are in the range $[-5, 5]$ (giving a total of 11^n lists for an input list of size n). For out-of-domain evaluation, we use lists of sizes 6 to 10 inclusive. Example scratchpads and zero-shot prompts are shown in Figure 12 and 11 respectively. The scratchpad is generated automatically through templates. We considered five exemplars for the few-shot setup.

B Experimental Setups & Empirical Results

B.1 Models

For our experiments, we evaluate the performance of 6 LLMs: GPT4 (gpt-4) [42], ChatGPT (GPT3.5-turbo) [41], GPT3 (text-davinci-003) [9], FlanT5 [14] and LLaMa [58]. The evaluations were conducted from January 2023 to May 2023 using the OpenAI API. We perform fine-tuning on GPT3 (text-davinci-003) for the three tasks, observing faster convergence when training on question-scratchpad pairs rather than question-answer pairs. For question-answer pairs fine-tuning, we train separately the model for {12, 12, 4} epochs for multiplication, puzzle, and DP respectively, saving the best model based on the validation set. Regarding training on question-scratchpad pairs, we train the model for {4, 8, 2} epochs for multiplication, puzzle, and DP. The batch size is set to approximately 0.2% of the number of examples in the training set. Generally, we observe that larger batch sizes tend to yield better results for larger datasets. For the learning rate multiplier, we experiment with values ranging from 0.02 to 0.2 to determine the optimal setting for achieving the best results and chose 0.2. During inference, we set nucleus sampling p to 0.7 and temperature to 1. For each task, we evaluate the performance of each model on 500 test examples.

B.2 Limits of Transformers in Zero- and Few-shot Settings

Figure 14, Figure 16 and Figure 18 show the zero-shot performance of GPT4, ChatGPT, LLaMA and FlanT5 on the three tasks. Overall, there is a notable decline in performance as the task complexity increases (measured by graph parallelism for multiplication and DP, and propagation steps for puzzles as shown in Figure 13). The few-shot performance with question-answer pairs results in minimal improvement over the zero-shot setting as depicted in Figure 15 and Figure 18 for the multiplication and DP tasks. In contrast, the few-shot setting did not lead to any improvement in the puzzle task.

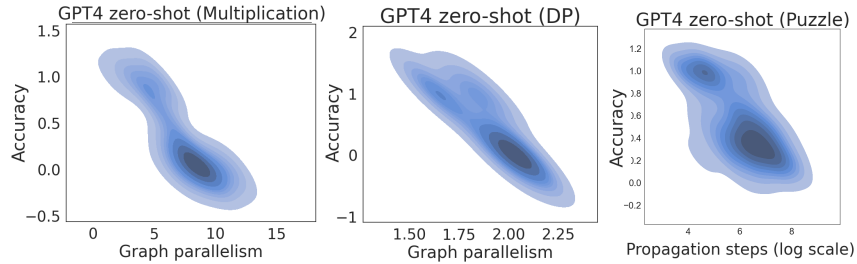


Figure 13: Graph parallelism vs accuracy. The accuracy decreases as the complexity increases.

ChatGPT zero-shot					GPT3 zero-shot					LLaMA zero-shot (13B)					FlanT5-XXL zero-shot (11B)				
1	2	3	4	5	1	2	3	4	5	1	2	3	4	5	1	2	3	4	5
1	0.99				1	0.88				0.6					0.96				
0.99	0.85	0.55			0.97	0.41	0.09			0.5	0.42				0.41	0.05			
0.98	0.51	0.11	0.01		0.85	0.28	0.04	0		0.22	0	0	0		0.15	0.02	0		
0.98	0.26	0.02	0	0	0.76	0.1	0	0	0	0	0	0	0		0.07	0	0	0	0

Figure 14: **Zero-shot accuracy.** Performance of ChatGPT, GPT3, LLaMA and FlanT5 on the **multiplication** task.

B.3 Limits of Transformers with question-answer Training

Figure 17 and Figure 19 show the performance of GPT3 finetuned on question-answer pairs. The model was trained on various splits, considering the problem size, depth, and width of the computation graph. Specifically, for the multiplication task, the model was fine-tuned on a range of multiplication problems, spanning from 1-digit by 1-digit multiplication to 4-digit by 2-digit multiplication amounting to 1.8M pairs. As for the puzzle task, the model was fine-tuned on puzzles of sizes ranging from 2x2 to 4x4 resulting in a total of 142k pairs. Additionally, for the DP task, the model was fine-tuned on problems with a sequence length of 5 resulting in 41K pairs. In an additional setup, we divided

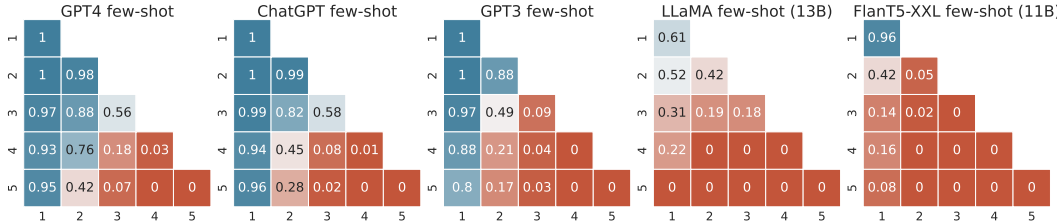


Figure 15: **Few-shot accuracy** with **question-answer** pairs. Performance of GPT4, ChatGPT, GPT3, LLaMA and FlanT5 on the **multiplication** task.

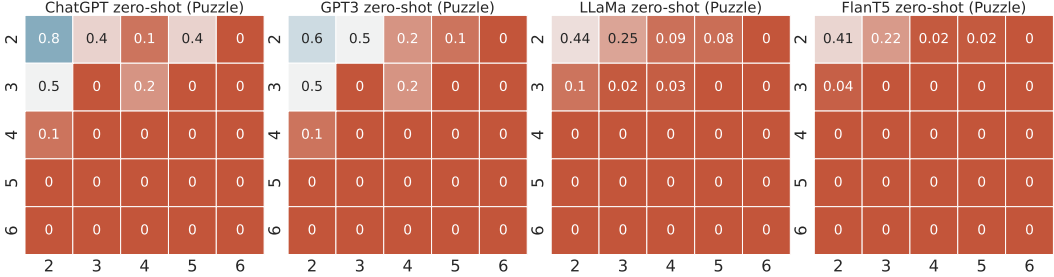


Figure 16: **Zero-shot accuracy**. Performance of ChatGPT, GPT3, LLaMA and FlanT5 on the **puzzle** task. Few-shot performance led to worse performance.

those datasets based on the depth and width of the computation graph for all the tasks and finetuned on different splits. The results indicate a lack of generalization for out-of-domain (OOD) examples while showcasing near-perfect performance for in-domain examples.

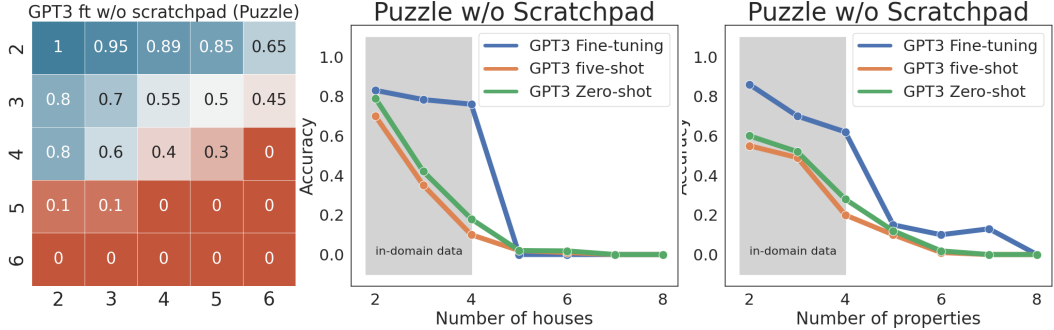


Figure 17: GPT3 finetuned on the puzzle task using **question-answer** pairs. The training data consisted of puzzles of size 4x4, and the model was subsequently evaluated on larger puzzle sizes for OOD testing.

GPT3 finetuning cost We will discuss here the approximate cost of fine-tuning GPT3 for the multiplication task. When fine-tuning with question-answer pairs, each example typically consists of around 20 tokens, and 250 tokens for question-scratchpad pairs. The cost for utilizing the `text-davinci-003` model amounts to \$0.02 (USD) per 1,000 tokens. With this particular setup, the total number of training examples required for multiplication up to 5 digits by 5 digits reaches an astonishing figure of approximately 9.1 billion examples. Should we choose to fine-tune GPT3 for 4 epochs on question-answer pairs, the cost would amount to \$12 million and \$700 million for question-scratchpad training. For a more comprehensive breakdown of the cost per problem size, please refer to Table 1.

B.4 Limits of Transformers with Explicit Scratchpad Training

Figure 21, 22, 20 show the performance of GPT3 finetuned on different splits of the tasks using question-scratchpad pairs. Specifically, for the multiplica-

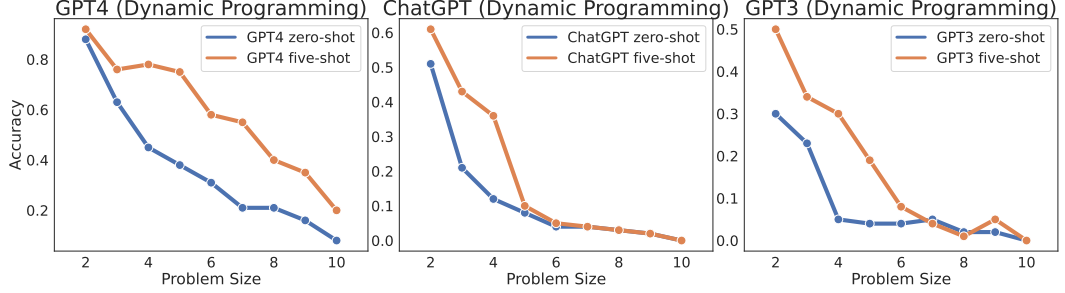


Figure 18: **Zero-shot and Few-shot accuracy using question-answer pairs.** Performance of GPT4, ChatGPT, and GPT3 on the **dynamic programming** task. LLaMA and FlanT5 results are near zero for all problem sizes.

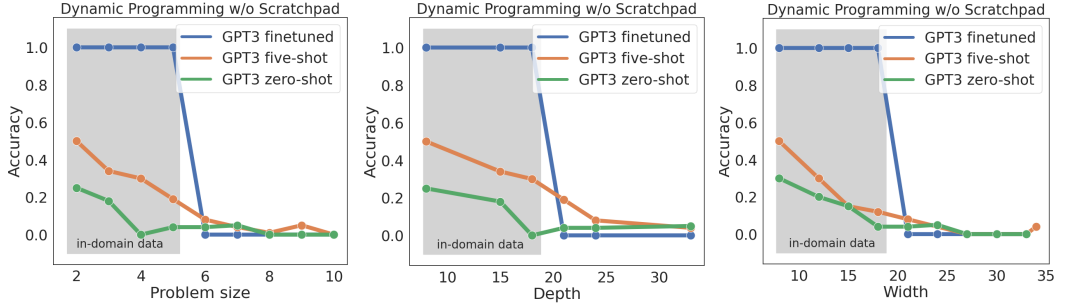


Figure 19: GPT3 finetuned on the **dynamic programming** task using **question-answer pairs**. We consider different data splits: problem size, depth, and width of the graph. Specifically, the model was trained with a problem size of 5, and the graph’s depth and width were set to 18.

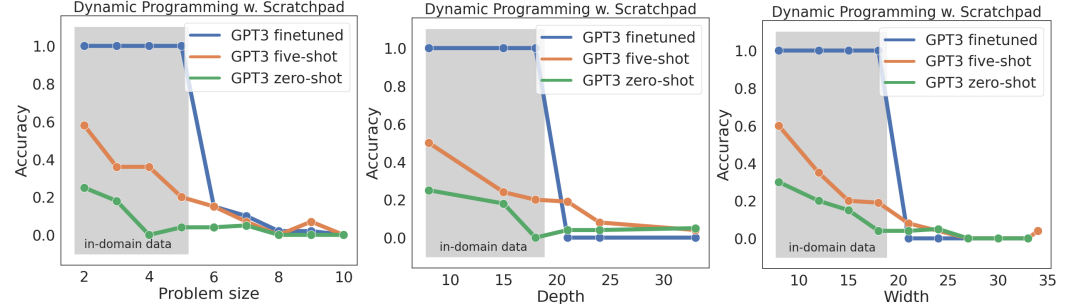


Figure 20: GPT3 finetuned on the **dynamic programming** task using **question-scratchpad pairs**. We consider different data splits: problem size, depth, and width of the graph. Specifically, the model was trained with a problem size of 5, and the graph’s depth and width were set to 18.

tion task, the model was fine-tuned on a range of multiplication problems, spanning from 1-digit by 1-digit multiplication to 3-digit by 2-digit multiplication.

As for the puzzle task, the model was fine-tuned on puzzles of sizes ranging from 2x2 to 4x4. Additionally, for the DP task, the model was fine-tuned on problems with a sequence length of 5. Furthermore, different data splits were considered, including variations based on the number of hours, number of properties, depth and width of the graph, and the number of digits in the multiplication output. On all tasks, we can see that the model fails to generalize to OOD data while achieving perfect accuracy on in-domain data, indicating that it cannot learn the underlying computational rules.

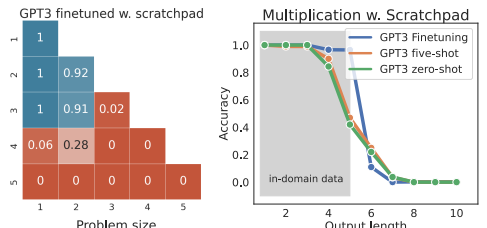


Figure 21: GPT3 finetuned exhaustively on task-specific data up to a certain problem size. In particular, we train on examples up to 3-digit by 2-digit multiplication (left) and on examples that have up to 5 digits in the output response (right). The **blue** region represents the in-distribution examples and the **red** region refers to OOD examples.

Problem size	# examples	GPT3 Cost	
		without scratchpad	with scratchpad
1 x 1	81	\$0.12	\$7.44
2 x 1	810	\$1.28	\$74.4
2 x 2	8100	\$12.96	\$744
3 x 1	8100	\$12.96	\$744
3 x 2	81000	\$129.6	\$7440
3 x 3	810000	\$1296	\$74,404
4 x 1	81000	\$129.6	\$7440
4 x 2	810000	\$1296	\$74,404
4 x 3	8100000	\$12,960	\$744,040
4 x 4	81000000	\$129,600	\$7,440,400
5 x 1	81000	\$1296	\$74,404
5 x 2	810000	\$12,960	\$744,040
5 x 3	8100000	\$129,600	\$7,440,400
5 x 4	81000000	\$1,296,000	\$70,440,400
5 x 5	810000000	\$12,960,000	\$700,440,400

Table 1: Finetuning cost of GPT3 model on the multiplication data.

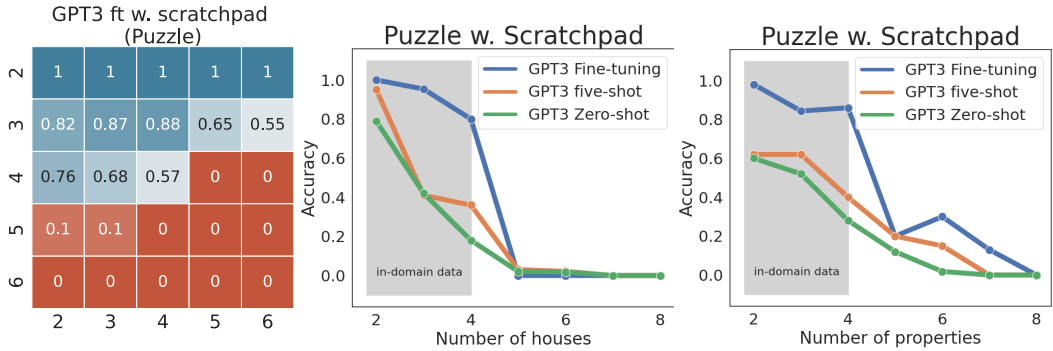


Figure 22: GPT3 finetuned on the puzzle task using **question-scratchpad** pairs. The training data consisted of puzzles of size 4x4, and the model was subsequently evaluated on larger puzzle sizes for OOD testing.

C Surface Patterns

C.1 Relative Information Gain Predictions for Multiplication

		Relative Information Gain			
Input variable	Output variable	2x2	3x3	4x4	5x5
x_n	z_{2n}	0.223	0.223	0.223	0.223
y_n	z_{2n}	0.223	0.223	0.223	0.223
x_1	z_1	0.198	0.199	0.199	0.199
y_1	z_1	0.198	0.199	0.199	0.199
$x_n y_n$	z_{2n}	1.000	1.000	1.000	1.000
$x_{n-1} x_n$	z_{2n}	0.223	0.223	0.223	0.223
$y_{n-1} y_n$	z_{2n}	0.223	0.223	0.223	0.223
$x_n y_n$	z_{2n-1}	0.110	0.101	0.101	0.101
$y_{n-1} y_n$	z_{2n-1}	0.032	0.036	0.036	0.036
$x_{n-1} x_n$	z_{2n-1}	0.032	0.036	0.036	0.036
$x_{n-1} y_{n-1}$	z_{2n-1}	0.018	0.025	0.025	0.025
$x_1 y_1$	z_2	0.099	0.088	0.088	0.088
$x_2 y_2$	z_2	0.025	0.016	0.016	0.016
$x_1 y_1$	z_1	0.788	0.792	0.793	0.793
$y_1 y_2$	z_1	0.213	0.211	0.211	0.211
$x_1 x_2$	z_1	0.213	0.211	0.211	0.211

Table 2: **Highest Relative Information Gain Elements and Pairs of Elements**, for multiplications between $x = (x_1, \dots, x_n)$ and $y = (y_1, \dots, y_n)$, with $2 \leq n \leq 5$. We define $z := x \cdot y$, which will always have size $2n$ (with possibly a leading zero). z_{2n} denotes the least-significant digit of z , and z_1 denotes the left-most digit. Only (input, output) pairs above 0.01 are shown. Note that since multiplication is commutative, several pairs of input variables (e.g. a_0 and b_0) exhibit the same relative information gain.

C.2 Empirical Surface Pattern Analysis for Multiplication with GPT4, ChatGPT and GPT3

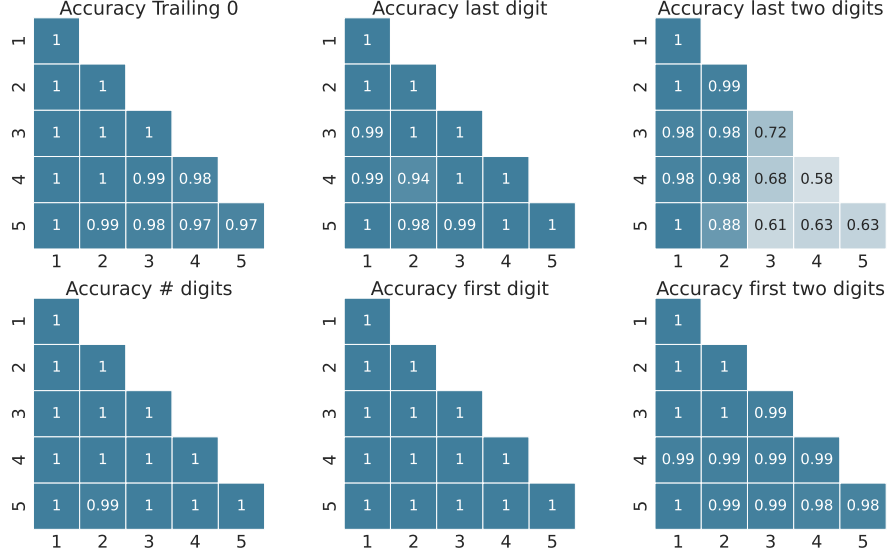


Figure 23: GPT4 zero-shot accuracy in predicting partially correct responses. This evidences surface pattern learning, since the accuracy of full answer prediction is significantly lower—and often near zero (see Figure 2). Specifically, ‘accuracy trailing zeros’ pertains to accurately predicting the number of zeros in the output number, which is known to be relatively easy to predict based on arithmetic calculations.

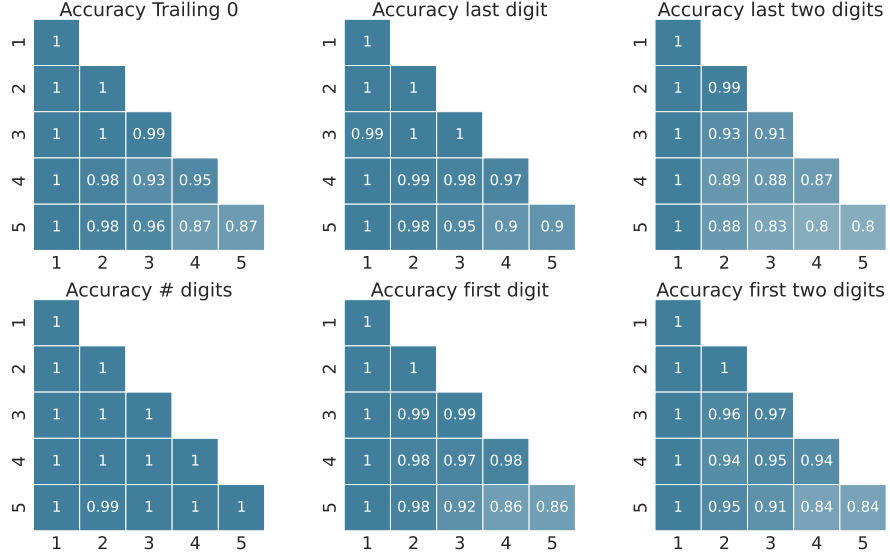


Figure 24: ChatGPT zero-shot accuracy in predicting partially correct responses. We observe the same trend for GPT3 predictions.

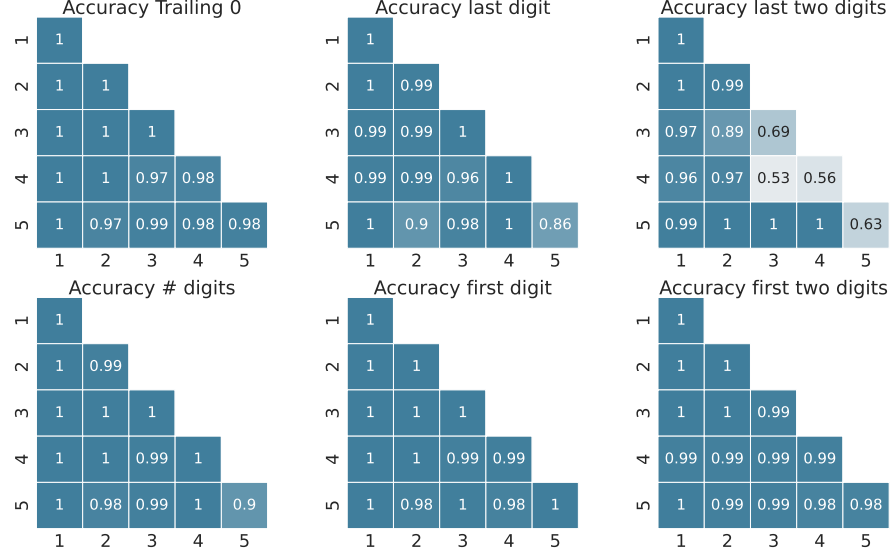


Figure 25: GPT4 five-shot accuracy in predicting partially correct responses. We observe the same trend for ChatGPT, GPT3 few-shot predictions.

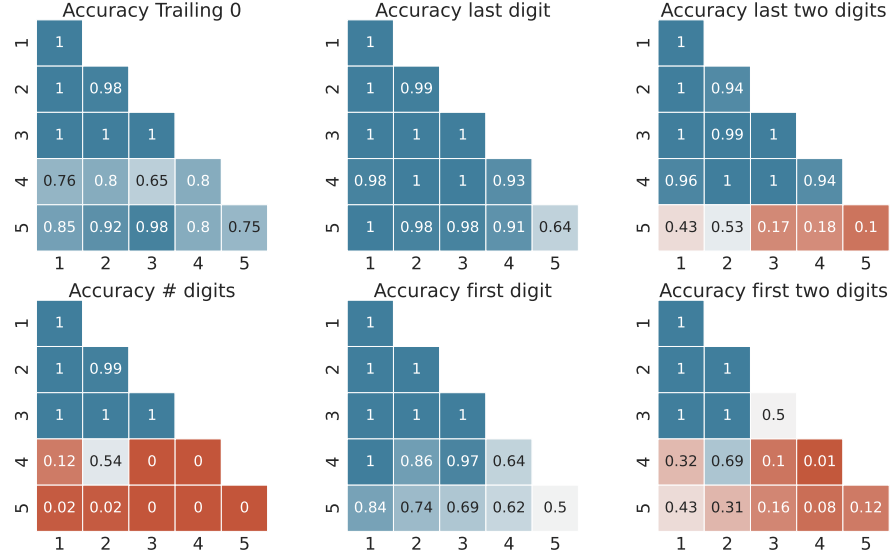


Figure 26: GPT3 finetuned on question-scratchpad pairs. Accuracy of predicting partially correct responses.

C.3 Relative Information Gain Predictions for Dynamic Programming Task

Let a_i be the i -th element of the input sequence, and let o_i be the i -th element of the output sequence. As shown in Table 3, a_i is a good predictor of o_i , and this is especially true for a_1 and a_{n-1} , the first and last elements of the sequence. This matches the task intuition, since one would never pick an element $a_i < 0$ and decrease the final sum (one may pick $a_i = 0$ if it makes a lexicographically smaller output sequence).

a_i weakly helps to predict its neighbors. The only case of this behavior with $\text{RelativeIG} > 0.1$ is at the start of the sequence, where the first element helps predict the value of the second. This again matches intuition, since a very high a_1 indicates that with high probability o_2 will not be selected for the final subsequence.

		Relative Information Gain for each problem size									
Input variable	Output variable	2	3	4	5	6	7	8	9	10	
a_1	o_2	0.15	0.13	0.14	0.14	0.14	0.14	0.14	0.14	0.14	
a_1	o_1	0.64	0.71	0.69	0.69	0.69	0.69	0.69	0.69	0.69	
a_2	o_2	0.53	0.42	0.45	0.44	0.45	0.44	0.44	0.45	0.44	
a_3	o_3	0.64	0.49	0.53	0.52	0.52	0.52	0.52	0.52	0.52	
a_4	o_4		0.60	0.46	0.50	0.49	0.49	0.49	0.49	0.49	
a_5	o_5			0.62	0.47	0.51	0.50	0.50	0.50	0.50	
a_6	o_6				0.61	0.47	0.51	0.49	0.50		
a_7	o_7					0.61	0.47	0.51	0.50		
a_8	o_8						0.61	0.47	0.51		
a_9	o_9							0.61	0.47		
a_{10}	o_{10}								0.61		
a_{n-1}	o_{n-1}	0.64	0.60	0.62	0.61	0.61	0.61	0.61	0.61		
a_{n-2}	o_{n-2}			0.46	0.47	0.47	0.47	0.47	0.47		
a_{n-3}	o_{n-3}					0.51	0.51	0.51	0.51		
a_{n-4}	o_{n-4}							0.49	0.50		

Table 3: **Highest Relative Information Gain Elements**, for DP problems of size $2 \leq n \leq 10$. We only show the (input, output) pairs where at least three problem sizes have $\text{RelativeIG} > 0$, and at least one with $\text{RelativeIG} > 0.1$. a_{n-1} refers to the last element of the sequence, regardless of its actual id in the sequence.

Similar behaviors, but with higher relative information gains overall, are observed when analyzing triples of consecutive elements in the list. Table 4 shows that o_i is highly predicted by (a_{i-1}, a_i, a_{i+1}) . Moreover, o_i is highly predicted by both (a_{i-2}, a_{i-1}, a_i) and (a_i, a_{i+1}, a_{i+2}) , with the former generally having higher scores than the latter. This again matches the task intuitions, since the value of the neighbors helps determine whether to select a number for the subsequence; and asking for the lexicographically smallest sequence biases the output subsequence to care more about the previous numbers rather than the following ones. We believe that this last point is the cause of the weakly predictive power of $(a_{i-3}, a_{i-2}, a_{i-1})$ to predict o_i ; whereas $(a_{i+1}, a_{i+2}, a_{i+3})$ is not shown, since all the relative information gain values were below 0.1.

		Relative Information Gain for each problem size							
Input variable	Output variable	3	4	5	6	7	8	9	10
$a_{n-3} a_{n-2} a_{n-1}$	o_{n-1}					0.95	0.95	0.95	0.95
$a_{n-3} a_{n-2} a_{n-1}$	o_{n-2}					0.87	0.87	0.87	0.87
$a_{n-3} a_{n-2} a_{n-1}$	o_{n-3}					0.64	0.64	0.64	0.64
$a_1 a_2 a_3$	o_1	1.00	0.96	0.97	0.97	0.97	0.97	0.97	0.97
$a_1 a_2 a_3$	o_2	1.00	0.91	0.92	0.91	0.92	0.91	0.92	0.91
$a_2 a_3 a_4$	o_2		0.56	0.55	0.55	0.55	0.55	0.55	0.56
$a_1 a_2 a_3$	o_3	1.00	0.66	0.73	0.71	0.72	0.72	0.72	0.72
$a_2 a_3 a_4$	o_3		0.86	0.77	0.78	0.78	0.78	0.78	0.78
$a_3 a_4 a_5$	o_3			0.67	0.66	0.66	0.66	0.66	0.66
$a_2 a_3 a_4$	o_4		0.94	0.64	0.7	0.68	0.69	0.69	0.69
$a_3 a_4 a_5$	o_4			0.88	0.79	0.81	0.8	0.8	0.8
$a_4 a_5 a_6$	o_4				0.63	0.62	0.62	0.62	0.62
$a_3 a_4 a_5$	o_5			0.95	0.65	0.71	0.69	0.7	0.7
$a_4 a_5 a_6$	o_5				0.87	0.78	0.79	0.79	0.79
$a_5 a_6 a_7$	o_5					0.64	0.63	0.63	0.64
$a_4 a_5 a_6$	o_6				0.94	0.64	0.71	0.69	0.7
$a_5 a_6 a_7$	o_6					0.87	0.78	0.8	0.8
$a_6 a_7 a_8$	o_6						0.64	0.62	0.63
$a_5 a_6 a_7$	o_7					0.95	0.64	0.71	0.69
$a_6 a_7 a_8$	o_7						0.87	0.78	0.8
$a_6 a_7 a_8$	o_8						0.95	0.64	0.71
$a_1 a_2 a_3$	o_4		0.12	0.1	0.11	0.11	0.11	0.11	0.11
$a_2 a_3 a_4$	o_5			0.1	0.09	0.1	0.09	0.1	0.1
$a_3 a_4 a_5$	o_6				0.11	0.1	0.1	0.1	0.11
$a_4 a_5 a_6$	o_7					0.11	0.09	0.1	0.11
$a_5 a_6 a_7$	o_7						0.11	0.09	0.11

Table 4: **Highest Relative Information Gain Contiguous Triples**, for DP problems of size $3 \leq n \leq 10$. We only show the (input, output) pairs where at least three problem sizes have $\text{RelativeIG} > 0$, and at least one with $\text{RelativeIG} > 0.1$. a_{n-1} refers to the last element of the sequence, regardless of its actual id in the sequence.

C.4 Empirical Surface Pattern Results for Dynamic Programming Task

We observe that all analyzed models match the Relative Information Gain prediction that o_1 (whether the first element goes into the output sequence or not) should be the easiest value to predict (see Figures 27, 28, and 29). However, since GPT3 often predicts shorter output sequences than the required size, the analysis of the predictive power of o_{n-1} is only done for GPT4. In GPT4, we observe that o_{n-1} is among the easiest values to predict as expected by Relative Information Gain.

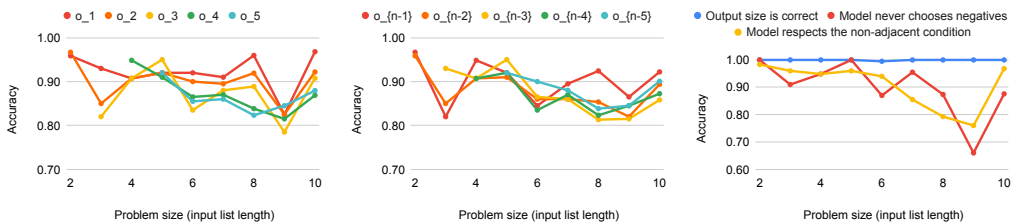


Figure 27: GPT4 five-shot with scratchpad accuracy in predicting output elements o_i in the DP task. All o_i are predicted with high accuracy with o_1 and o_{n-1} being consistently among the highest. These observations go in line with the Relative Information Gain prediction.

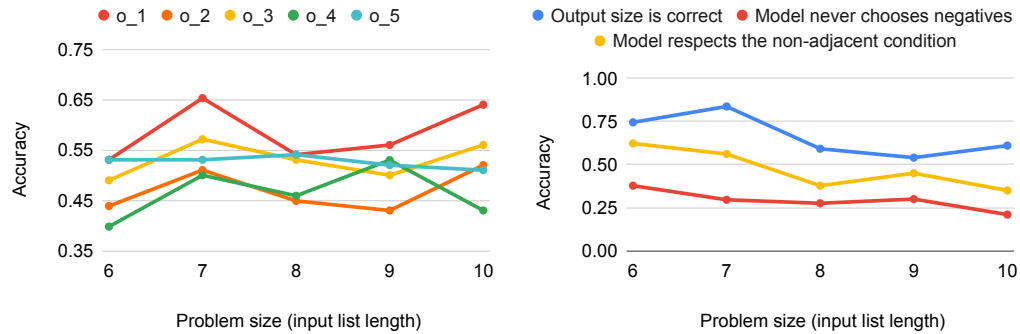


Figure 28: GPT3 few-shot without scratchpad accuracy in predicting output elements o_i in the DP task. As predicted by Relative Information Gain, the model predicts o_1 correctly with the highest probability. However, because GPT3 often does not produce the correct output size, it hinders us from analyzing o_{n-1} .

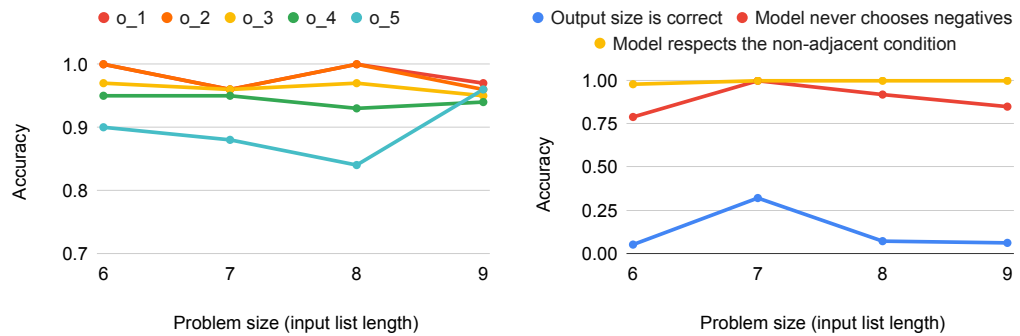


Figure 29: GPT3 fine-tuned without scratchpad accuracy in predicting output elements o_i in the DP task. As predicted by Relative Information Gain, the model predicts o_1 correctly with the highest probability. However, because GPT3 often does not produce the correct output size, it hinders us from analyzing o_{n-1} .

D Theoretical Results: Derivations

D.1 Transformers struggle with problems with increasingly larger parallelism (*width*)

Proposition D.1. Let $f_n(\mathbf{x}) = h_n(g(\mathbf{x}, 1), g(\mathbf{x}, 2), \dots, g(\mathbf{x}, n))$. Let $\hat{h}_n, \hat{g}, \hat{f}_n$ be estimators of h_n, g, f_n respectively. Assume $\mathbb{P}(h_n = \hat{h}_n) = 1$ and $\mathbb{P}(h_n(X) = h_n(Y) \mid X \neq Y) < \beta\alpha^n$ for some $\alpha \in (0, 1)$ and $\beta > 0$ (i.e. \hat{h}_n perfectly estimates h_n , and h_n is almost injective). If $\mathbb{P}(g \neq \hat{g}) = \epsilon > 0$ and errors in \hat{g} are independent, then $\lim_{n \rightarrow +\infty} \mathbb{P}(f_n \neq \hat{f}_n) = 1$.

Proof. For ease of writing, let $X_i = g(X, i)$ and $Y_i = \hat{g}(X, i)$, and let $\mathbf{X} = (X_1, \dots, X_n)$ and $\mathbf{Y} = (Y_1, \dots, Y_n)$. We will compute some auxiliary probabilities, and then upper bound $\mathbb{P}(f = \hat{f})$, to finally compute its limit.

$$\begin{aligned} \mathbb{P}(\mathbf{X} = \mathbf{Y}) &= \mathbb{P}(X_1 = Y_1, X_2 = Y_2, \dots, X_n = Y_n) \\ &= \mathbb{P}(X_1 = Y_1) \cdot \mathbb{P}(X_2 = Y_2) \cdots \mathbb{P}(X_n = Y_n) = \mathbb{P}(g = \hat{g})^n = (1 - \epsilon)^n \end{aligned} \quad (2)$$

Since by hypothesis we know $\mathbb{P}(h_n(\mathbf{Y}) = \hat{h}_n(\mathbf{Y})) = 1$, we have that:

$$\begin{aligned} \mathbb{P}(h_n(\mathbf{X}) = \hat{h}_n(\mathbf{Y}) \mid \mathbf{X} \neq \mathbf{Y}) &= \mathbb{P}(h_n(\mathbf{X}) = \hat{h}_n(\mathbf{Y}) \cap h_n(\mathbf{Y}) = \hat{h}_n(\mathbf{Y}) \mid \mathbf{X} \neq \mathbf{Y}) \\ &= \mathbb{P}(h_n(\mathbf{X}) = h_n(\mathbf{Y}) = \hat{h}_n(\mathbf{Y}) \mid \mathbf{X} \neq \mathbf{Y}) \\ &\leq \mathbb{P}(h_n(\mathbf{X}) = h_n(\mathbf{Y}) \mid \mathbf{X} \neq \mathbf{Y}) \\ &< \beta\alpha^n \end{aligned} \quad (3)$$

We will now estimate $\mathbb{P}(f_n = \hat{f}_n)$ using the law of total probability w.r.t. the event $\mathbf{X} = \mathbf{Y}$.

$$\begin{aligned} \mathbb{P}(f_n = \hat{f}_n) &= \mathbb{P}(h_n(\mathbf{X}) = \hat{h}_n(\mathbf{Y})) \\ &= \mathbb{P}(h_n(\mathbf{X}) = \hat{h}_n(\mathbf{Y}) \mid \mathbf{X} = \mathbf{Y}) \cdot \mathbb{P}(\mathbf{X} = \mathbf{Y}) + \mathbb{P}(h_n(\mathbf{X}) = \hat{h}_n(\mathbf{Y}) \mid \mathbf{X} \neq \mathbf{Y}) \cdot \mathbb{P}(\mathbf{X} \neq \mathbf{Y}) \\ &= \mathbb{P}(h_n(\mathbf{X}) = \hat{h}_n(\mathbf{X})) \cdot \mathbb{P}(\mathbf{X} = \mathbf{Y}) + \mathbb{P}(h_n(\mathbf{X}) = \hat{h}_n(\mathbf{Y}) \mid \mathbf{X} \neq \mathbf{Y}) \cdot (1 - \mathbb{P}(\mathbf{X} = \mathbf{Y})) \\ &= 1 \cdot (1 - \epsilon)^n + \mathbb{P}(h_n(\mathbf{X}) = \hat{h}_n(\mathbf{Y}) \mid \mathbf{X} \neq \mathbf{Y}) \cdot (1 - (1 - \epsilon)^n) \quad (\text{using 2 and hypothesis}) \\ &< (1 - \epsilon)^n + \beta\alpha^n \cdot (1 - (1 - \epsilon)^n) \quad (\text{using 3}) \\ &< \beta\alpha^n + (1 - \epsilon)^n \cdot (1 - \beta\alpha^n) \end{aligned}$$

To conclude our proof, we will show that $\lim_{n \rightarrow +\infty} \mathbb{P}(f_n = \hat{f}_n)$ exists and compute its value. Note that since $1 - \epsilon \in [0, 1)$ and $\alpha \in (0, 1)$, trivially $\lim_{n \rightarrow +\infty} \beta\alpha^n + (1 - \epsilon)^n \cdot (1 - \beta\alpha^n) = 0$.

$$0 \leq \liminf_{n \rightarrow +\infty} \mathbb{P}(f_n = \hat{f}_n) \leq \limsup_{n \rightarrow +\infty} \mathbb{P}(f_n = \hat{f}_n) \leq \limsup_{n \rightarrow +\infty} \beta\alpha^n + (1 - \epsilon)^n \cdot (1 - \beta\alpha^n) = 0$$

Then, $\lim_{n \rightarrow +\infty} \mathbb{P}(f_n = \hat{f}_n) = 0$ and we conclude $\lim_{n \rightarrow +\infty} \mathbb{P}(f_n \neq \hat{f}_n) = 0$. \square

Corollary D.1. Assume that a model \mathcal{M} solves shifted addition perfectly, but it incorrectly solves **at least one** m digit by 1 digit multiplication for some fixed m . Then, the probability that \mathcal{M} will solve any m digit by n digit multiplication using the long-form multiplication algorithm tends to 0.

Proof. We define $s : \mathbb{Z}_{10}^{m+n} \times \mathbb{N} \rightarrow \mathbb{N} \times \mathbb{N}$, $d : \mathbb{N} \times \mathbb{Z}_{10} \rightarrow \mathbb{N}$, $h_n : \mathbb{N}^n \rightarrow \mathbb{N}$, and $f_n : \mathbb{Z}_{10}^{m+n} \rightarrow \mathbb{N}$ as follows.

$$\begin{aligned} s([x_1, \dots, x_m, x_{m+1}, \dots, x_{m+n}], j) &:= (x_1 \widehat{\ } x_2 \widehat{\ } \dots \widehat{\ } x_m, x_{m+j}) \\ &\quad \text{where } x_1 \widehat{\ } x_2 \widehat{\ } \dots \widehat{\ } x_m \text{ denotes concatenating digits } x_i \\ d(x, y) &:= x \cdot y \\ g &:= d \circ s \\ h_n(x_1, \dots, x_n) &:= \sum_{i=1}^n x_i 10^{n-i} \\ f_n(\mathbf{x}) &:= h_n(g(\mathbf{x}, 1), g(\mathbf{x}, 2)), \dots, g(\mathbf{x}, n) \end{aligned}$$

Note that g defines the base-10 multiplication between m -digit numbers $(x_1 x_2 \dots x_m)$ and 1-digit numbers (x_{m+j}) , where s denotes the selection of the numbers to multiply and d denotes the actual multiplication. Note that h_n describes the shifted addition used at the end of long-form multiplication to combine n m -digit by 1-digit multiplications. Therefore, f_n describes the long-form multiplication of m -digit by n -digit numbers.

By hypothesis, $\mathbb{P}(g \neq \hat{g}) = \epsilon > 0$ and $\mathbb{P}(h_n = \hat{h}_n) = 1$, where \hat{g} and \hat{h}_n denote estimators using model \mathcal{M} . It can be shown that $\mathbb{P}(h_n(X) = h_n(Y) \mid X \neq Y) < \beta\alpha^n$ for $\alpha = 0.1$ and $\beta = 10^m$. Using Lemma D.1, $\lim_{n \rightarrow +\infty} \mathbb{P}(f_n \neq \hat{f}_n) = 1$, which concludes our proof.

□

Note that Lemma D.1's proofs gives us empirical bounds once ϵ and α are approximated. Also **note that our definition of g in the proof of Corollary D.1 highlights two possible sources of exponentially-accumulating error:** errors in the selection of the numbers to multiply s , and errors in the actual m -digit by 1-digit multiplication d .

D.2 Transformers struggle with problems that require increasingly larger iterative applications of a function (*depth*)

Proposition D.2. Let $f_n(\mathbf{x}) = g^n(\mathbf{x})$. Assume $\mathbb{P}(g(X) = \hat{g}(Y) \mid X \neq Y) \leq c$ (i.e. recovering from a mistake due to the randomness of applying the estimator on an incorrect input has probability at most c). If $\mathbb{P}(g \neq \hat{g}) = \epsilon > 0$ with $c + \epsilon < 1$, then $\liminf_{n \rightarrow +\infty} \mathbb{P}(f_n \neq \hat{f}_n) = 1 - \frac{c}{c + \epsilon}$.

Proof. We first derive a recursive upper bound using the law of total probability, and then prove a non-recursive upper bound by induction.

$$\begin{aligned} s_n := \mathbb{P}(f_n = \hat{f}_n) &= \mathbb{P}(g(g^{n-1}(Z)) = \hat{g}(\hat{g}^{n-1}(Z))) \\ &= \mathbb{P}(g(\mathbf{X}) = \hat{g}(\mathbf{Y})) \quad \text{where } \mathbf{X} := g^{n-1}(Z) \text{ and } \mathbf{Y} := \hat{g}^{n-1}(Z) \\ &= \mathbb{P}(g(\mathbf{X}) = \hat{g}(\mathbf{Y}) \mid \mathbf{X} = \mathbf{Y}) \cdot \mathbb{P}(\mathbf{X} = \mathbf{Y}) + \mathbb{P}(g(\mathbf{X}) = \hat{g}(\mathbf{Y}) \mid \mathbf{X} \neq \mathbf{Y}) \cdot \mathbb{P}(\mathbf{X} \neq \mathbf{Y}) \\ &= \mathbb{P}(g(\mathbf{X}) = \hat{g}(\mathbf{X})) \cdot \mathbb{P}(\mathbf{X} = \mathbf{Y}) + \mathbb{P}(g(\mathbf{X}) = \hat{g}(\mathbf{Y}) \mid \mathbf{X} \neq \mathbf{Y}) \cdot (1 - \mathbb{P}(\mathbf{X} = \mathbf{Y})) \\ &= \mathbb{P}(g(\mathbf{X}) = \hat{g}(\mathbf{X})) \cdot s_{n-1} + \mathbb{P}(g(\mathbf{X}) = \hat{g}(\mathbf{Y}) \mid \mathbf{X} \neq \mathbf{Y}) \cdot (1 - s_{n-1}) \\ &\leq (1 - \epsilon) \cdot s_{n-1} + c \cdot (1 - s_{n-1}) \\ &\leq (1 - \epsilon - c) \cdot s_{n-1} + c \end{aligned}$$

We know $s_1 = (1 - \epsilon)$ since $s_1 = \mathbb{P}(f_1 = \hat{f}_1) = \mathbb{P}(g = \hat{g})$. Let $b := 1 - \epsilon - c$ for ease of writing. Then, we have

$$s_n \leq b \cdot s_{n-1} + c \tag{4}$$

It can be easily shown by induction that $s_n \leq b^{n-1}(1 - \epsilon) + c \sum_{i=0}^{n-2} b^i$:

- The **base case** $n = 2$ is true since we know $s_2 \leq b \cdot s_1 + c$, and $b \cdot s_1 + c = b(1 - \epsilon) + c = b^{2-1}(1 - \epsilon) + c \sum_{i=0}^{2-2} b^i$, thus showing $s_2 \leq b^{2-1}(1 - \epsilon) + c \sum_{i=0}^{2-2} b^i$
- The **inductive step** yields directly using Equation 4,

$$\begin{aligned} s_n &\leq b \cdot s_{n-1} + c \\ &\leq b \cdot \left(b^{n-2}(1 - \epsilon) + c \sum_{i=0}^{n-3} b^i \right) + c \leq b^{n-1}(1 - \epsilon) + c \sum_{i=1}^{n-2} b^i + c \leq b^{n-1}(1 - \epsilon) + c \sum_{i=0}^{n-2} b^i \end{aligned}$$

We can rewrite the geometric series $\sum_{i=0}^{n-2} b^i$ in its closed form $\frac{1-b^{n-1}}{1-b}$, and recalling $b := 1 - \epsilon - c$,

$$\begin{aligned} s_n &\leq b^{n-1}(1 - \epsilon) + c \frac{1 - b^{n-1}}{1 - b} = b^{n-1}(1 - \epsilon) + c \frac{1 - b^{n-1}}{c + \epsilon} \\ &= b^{n-1}(1 - \epsilon) + \frac{c}{c + \epsilon} - b^{n-1} \frac{c}{c + \epsilon} \\ &= b^{n-1} \left(1 - \epsilon - \frac{c}{c + \epsilon} \right) + \frac{c}{c + \epsilon} \end{aligned}$$

Recalling that $s_n = \mathbb{P}(f_n = \hat{f}_n)$, we compute the limit inferior of $\mathbb{P}(f_n \neq \hat{f}_n) = 1 - s_n \geq 1 - b^{n-1} \left(1 - \epsilon - \frac{c}{c+\epsilon}\right) - \frac{c}{c+\epsilon}$.

$$\liminf_{n \rightarrow +\infty} \mathbb{P}(f_n \neq \hat{f}_n) \geq \lim_{n \rightarrow +\infty} 1 - b^{n-1} \left(1 - \epsilon - \frac{c}{c+\epsilon}\right) - \frac{c}{c+\epsilon} = 1 - \frac{c}{c+\epsilon}$$

that concludes our proof. \square

We can generalize the proof in Lemma 4.2 to tasks where there are potentially many valid reasoning chains with the following alternative state-transition framing.

Lemma D.2. *Let S denote the set of all possible states a language model can generate, and let $z : S \rightarrow \{0, 1\}$ defines if a state is valid ($0 = \text{invalid}$). Let $\hat{g} : S \rightarrow \Pi(S)$ be a state-transition function representing a language model's probability distribution of generating each possible next state when attempting to perform a single reasoning step. Assume $\mathbb{P}(z(\hat{g}(X)) = 1 | z(X) = 0) \leq \frac{c}{c+\epsilon}$ and $\mathbb{P}(z(\hat{g}(X)) = 0 | z(X) = 1) = \epsilon > 0$ with $c + \epsilon < 1$. Then, $\liminf_{n \rightarrow +\infty} \mathbb{P}(z(\hat{g}^n) = 0) = 1 - \frac{c}{c+\epsilon}$.*

If for task T we know that all valid reasoning chains to arrive at a correct result have at least length n (i.e., the equivalent of defining $f_n = g^n$ in Lemma D.1) then the probability of solving task T correctly tends to at most $\frac{c}{c+\epsilon}$.

Corollary D.3. *The recursions for dynamic programming tasks, the m -by-1 digit multiplication, and the puzzle's elimination function are all tasks where there is a fixed reasoning step g being repeatedly applied. Therefore, we can directly apply Proposition 4.2 to these tasks.*

Proof. Let's analyze the three tasks separately below.

m -by-1 digit multiplication may be viewed as $f^m(\mathbf{x})$ Let $x = (x_1, \dots, x_m)$ be the m -digit number that we multiply by the 1-digit number y ($0 \leq y < 10$). Let $z = (z_1, \dots, z_{m+1})$ denote $z = x \cdot y$, which is guaranteed to have exactly $m + 1$ digits (with possibly leading zeros). We define f as:

$$f(x_1, \dots, x_m, y, i, c) := (x_1, \dots, x_{i-1}, x'_i, x_{i+1}, \dots, x_m, y, i-1, c')$$

where $x'_i := (x_i \cdot y + c) \bmod 10$ and $c' := \lfloor (x_i \cdot y + c)/10 \rfloor$. Note that $x'_i = z_{i+1}$ since f is performing one step of the long-form multiplication algorithm.

Let the initial input be $\mathbf{x} := (x_1, \dots, x_m, y, m, 0)$. Then, it can be easily shown that $f^m(\mathbf{x}) = (z_2, \dots, z_{m+1}, y, 0, c)$. Since c is the left-most carry, it is the leading digit of z , i.e. $c = z_1$ (possibly zero). Thus, the value of z can be directly extracted from $f^m(\mathbf{x}) = (z_2, \dots, z_{m+1}, y, 0, z_1)$.

In the DP task, dp 's computation may be viewed as $f^{m-2}(\mathbf{x})$ for a list of size m See §A.3.1 for details on the solution to this problem. We will use identical notation. Let a_1, \dots, a_m be an input list. Let $\mathbf{x} = (a_1, \dots, a_{m-2}, a'_{m-1}, a'_m, m-2)$, where $a'_m := \max(a_m, 0)$ and $a'_{m-1} := \max(a_{m-1}, a_m, 0)$. Intuitively, this means that we have applied the first two steps of the dp computation, and stored the results in a'_{m-1} and a'_m . Let f be a function representing the recursive computation of dp_i :

$$f(a_1, \dots, a_i, a'_{i+1}, \dots, a'_m, i) = (a_1, \dots, a_{i-1}, a'_i, \dots, a'_m, i-1)$$

where $a'_i := \max(a'_{i+1}, a_i + a'_{i+2}, 0)$.

Note that since a'_{i+1} stores the value of dp_{i+1} and a'_{i+2} stores the value of dp_{i+2} , it can be easily shown that $f^{m-2}(\mathbf{x}) = (a'_1, \dots, a'_m, 0) = (dp_1, \dots, dp_m, 0)$. Therefore, f^{m-2} computes all recursive values of dp_i when given the base cases.

In the DP task, the reconstruction of the desired subsequence given already computed dp values may be viewed as $f^m(\mathbf{x})$ for an input list of size m . This case is similar to the previous one. Let $r = (r_1, \dots, r_m)$ be the result, where $r_i = 1$ if a_i was selected for the desired subsequence, and $r_i = 2$ otherwise. Let $\mathbf{x} := (dp_1, \dots, dp_m, 0, 0, a_1, \dots, a_m, 1, 1)$. Let f be defined as follows:

$$f(dp_1, \dots, dp_m, 0, 0, a'_1, \dots, a'_{i-1}, a_i, \dots, a_m, i, u) = (dp_1, \dots, dp_m, 0, 0, a'_1, \dots, a'_i, a_{i+1}, \dots, a_m, i+1, u')$$

where $a'_i := 2 - \mathbb{1}\{dp_i = a_i + dp_{i+2} \text{ and } u = 1\}$ and $u := 1 - \mathbb{1}\{dp_i = a_i + dp_{i+2} \text{ and } u = 1\}$. Intuitively, a'_i stores whether the i -th element of the list should be selected for the final subsequence, assigning 1 if the element should be taken, and 2 otherwise (i.e., $a'_i = r_i$). Moreover, if the i -th element has been selected, we mark that the next item will not be available using u' . Therefore, f performs one step of the final output reconstruction as defined in §A.3.1.

It can be easily shown that $f^m(\mathbf{x}) := (dp_1, \dots, dp_m, 0, 0, a'_1, \dots, a'_m, m+1, u') = (dp_1, \dots, dp_m, 0, 0, r_1, \dots, r_m, m+1, u')$. Note that the extra two elements in the input state allow lifting the special cases $m-1$ and m in the solution shown in §A.3.1 without falling out of bounds.

Solving the puzzle task may be seen as f^m for some m , where f is the elimination function Let c_1, \dots, c_n be the list of clues, let H be the number of houses, and let A be a partially filled solution of size $K \times M$ as defined in §2.4. Each cell A_{ij} can take $H+1$ values: the H options for the cell and the value \emptyset , implying this cell has not been filled. An elimination step f may be defined as:

$$f(c_1, \dots, c_n, A_{11}, \dots, A_{1M}, \dots, A_{K1}, \dots, A_{KM}) = (c_1, \dots, c_n, A'_{11}, \dots, A'_{1M}, \dots, A'_{K1}, \dots, A'_{KM})$$

where A' is also a partially filled matrix, with $A_{ij} = A'_{ij}$ for every $A_{ij} \neq \emptyset$ and where A' has at least one more filled cell.

Let $\mathbf{x} = (c_1, \dots, c_n, E)$ where E is an empty matrix of size $K \times M$ (all cell values of E are \emptyset).

Then, a full solution is computed as $f^m(\mathbf{x})$ for some value of m that increases with the problem size. In contrast to other tasks, the value of m is not fixed, and depends on the task instance, but using solvers we know that m increases with problem size. \square

D.3 Discussing $c \ll \epsilon$ in the context of Proposition 4.2

Note that in Proposition 4.2, if $c \ll \epsilon$ then $\liminf_{n \rightarrow +\infty} \mathbb{P}(f_n \neq \hat{f}_n) \approx 1$. This is because assuming $\epsilon = m \cdot c$ for some $m > 0$, we have $1 - \frac{c}{c+\epsilon} = 1 - \frac{c}{c+m \cdot c} = 1 - \frac{1}{m+1} = \frac{m}{m+1}$, and $\frac{m}{m+1}$ is a monotonically increasing function for all $m > 0$ that tends to 1 when m goes to infinity. Therefore, large m 's (or alternatively, $c \ll \epsilon$) imply $\frac{m}{m+1}$ will be close to 1.

It is reasonable to assume $c \ll \epsilon$ when g has low collision, since c represents the probability of the estimator $\hat{g}(y)$ arriving at the correct output $g(x)$ by chance when given the wrong input $y \neq x$.

If g is discrete, it can take $|\text{Im}(g)|$ values, where $|\text{Im}(g)|$ denotes the cardinal of the image space of g . Assuming approximately uniform errors, $c \approx \epsilon / |\text{Im}(g)|$, which in turn implies $c \ll \epsilon$ since g being low collision implies $|\text{Im}(g)|$ is large.

If g is continuous, then assuming approximately uniform errors we have $c \approx 0$.

Summarizing both cases, if errors are approximately evenly distributed we obtain that $\liminf_{n \rightarrow +\infty} \mathbb{P}(f_n \neq \hat{f}_n) \approx 1$.

D.4 Error rates in repeated applications of a function may be unbounded

Time series analysis studies series $(y_t)_t$ where each y_t linearly depends on the immediately previous $p \geq 1$ time steps, and potentially including an error component. We will focus on the vectorial case, defined as follows.

Definition D.1 (Hamilton 1994, p -th order vector autorregressions, VAR(p)). *Let*

$$y_t = c + \Phi_1 y_{t-1} + \Phi_2 y_{t-2} + \dots + \Phi_p y_{t-p} + \epsilon_t$$

where c denotes a $n \times 1$ vector of constants and Φ_i denotes an $n \times n$ matrix of autoregressive coefficients. The $n \times 1$ ϵ_t vector is a generalization of white noise: $E(\epsilon_t) = 0$, $E(\epsilon_t, \epsilon_\Gamma') = 0$ for $\Gamma \neq \Gamma$, and $E(\epsilon_t, \epsilon_t) = \Omega$ with Ω symmetric positive definite matrix.

We say a process is covariance-stationary if its first and second moments ($E[y_t]$ and $E[y'_{t-j}]$) are independent of the time t . Intuitively, this implies that the consequences of any ϵ_t must eventually die out. Such a process may also be referred to as a *stable process* (e.g., in Lütkepohl 2005). The following necessary and sufficient condition for stableness can be derived:

Proposition D.3 (Hamilton 1994, Proposition 10.1). *Let F be an $np \times np$ matrix defined as follows.*

$$F = \begin{bmatrix} \Phi_1 & \Phi_2 & \Phi_3 & \dots & \Phi_{p-1} & \Phi_p \\ I_n & 0 & 0 & \dots & 0 & 0 \\ 0 & I_n & 0 & \dots & 0 & 0 \\ 0 & 0 & I_n & \dots & 0 & 0 \\ 0 & 0 & 0 & \dots & I_n & 0 \end{bmatrix}$$

The eigenvalues of matrix F satisfy

$$|I_n \lambda^p - \Phi_1 \lambda^{p-1} - \Phi_2 \lambda^{p-2} - \dots - \Phi_p| = 0$$

Hence, a VAR(p) is covariance-stationary as long as $|\lambda| < 1$ for all values of λ satisfying this equation.

In our case, repeated iterations only involve considering the immediately previous step, i.e. $p = 1$. Then, a VAR(1) process $y_t = c + \Phi_1 y_{t-1} + \epsilon_t$ is covariance-stationary (or stable) if and only if the eigenvalues of $F = \Phi_1$ lie inside the unit circle. F will be unstable if at least one eigenvalue lies outside the unit circle, which in turn usually means an explosive system.

Intuition For VAR(1) (i.e., $y_t = c + \Phi_1 y_{t-1} + \epsilon_t$), we can intuitively see why large eigenvalues are problematic. If y_t is VAR(1), then it can be rewritten as

$$y_t = \Phi_1^t y_0 + \sum_{i=1}^{t-1} \Phi_1^i \epsilon_{t-i} + \left(I_n + \sum_{i=0}^{t-1} \Phi_1^i \right) c$$

Intuitively, large eigenvalues are problematic because if we diagonalize $\Phi_1 = PDP^{-1}$, then $\Phi_1^t = PD^t P^{-1}$, with $D_{ii} = \lambda_i^t$. Thus, a component of Φ_1^t will diverge if $|\lambda_i| > 1$. If Φ_1 is not diagonalizable, a similar argument holds for its Jordan decomposition. See Lütkepohl 2005, Section 2.1.1 for details.

E Societal impact

Our work on analyzing the limitations of current Transformers in compositional tasks can have a positive societal impact in several ways. By shedding light on these limitations, we contribute to a deeper understanding of the capabilities and constraints of these models. This knowledge is essential for researchers, developers, and policymakers in making informed decisions regarding the application of Transformers in various domains.

Understanding the limitations of Transformers in compositional reasoning is crucial for developing more reliable and robust AI systems. By identifying these shortcomings, we can direct future research efforts toward addressing these limitations and developing models that exhibit improved performance in handling complex tasks requiring compositional reasoning.

We do not foresee any negative societal impacts, as our analysis aims to understand the reasons behind transformers' failures and successes, but does not introduce any new model or dataset that future work may leverage.